

Electronic Supplementary Information (ESI)

Thioalkyl- and Sulfone-Substituted Poly(*p*-Phenylene Vinylene)s

Martina Rimmele,^a Klaus Ableidinger,^a Adam V. Marsh,^b Nathan J. Cheetham,^c M. Josef Taublaender,^{a,d} Alina Buchner,^a Jonathan Prinz,^a Johannes Fröhlich,^a Miriam M. Unterlass,^{a,d} Martin Heeney,^b Florian Glöcklhofer^{a,b,*}

^a Institute of Applied Synthetic Chemistry, TU Wien, Getreidemarkt 9/163,
1060 Vienna, Austria.

^b Department of Chemistry and Centre for Plastic Electronics, Imperial College London,
London W12 0BZ, UK.

^c Department of Physics and Centre for Plastic Electronics, Imperial College London,
London SW7 2AZ, UK.

^d Institute of Materials Chemistry, TU Wien, Getreidemarkt 9/165, 1060 Vienna, Austria.

* f.glocklhofer@imperial.ac.uk

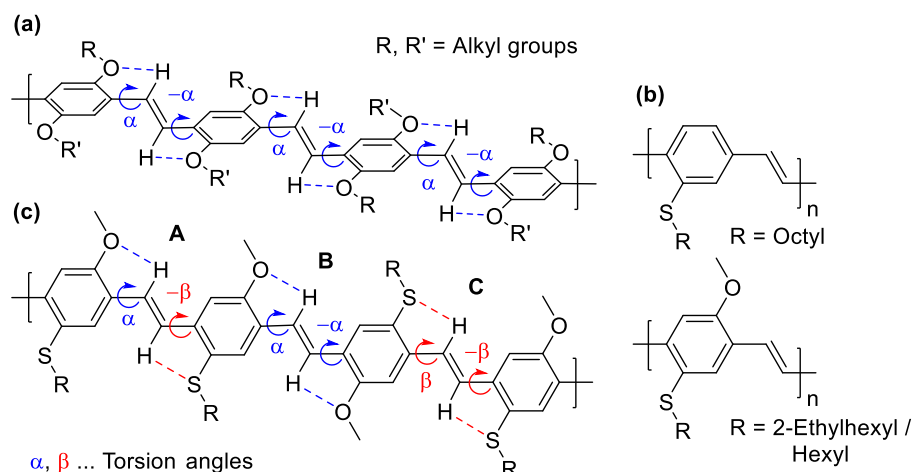
Table of Contents

1. Conformational effects.....	1
2. ¹ H and ¹³ C(APT) NMR spectra	3
3. Gel permeation chromatography (GPC).....	21
4. Elemental analysis.....	22
5. Infrared (IR) spectra	22
6. Thermogravimetric analysis (TGA) and differential scanning calorimetry (DSC).....	23
7. Cyclic voltammetry (CV)	24
8. Photophysical measurements	25
8.1. UV-vis absorption and photoluminescence (PL) in solution	25
8.2. UV-vis absorption and photoluminescence (PL) spectra of thin-films.....	26
8.3. Photoluminescence quantum efficiency (PLQE) in the solid state	26
9. Equation for DMDO concentration calculation	26
10. Other syntheses.....	27
10.1. Synthesis of 1-bromo-3,7-dimethyloctane	27
10.2. Synthesis of 3,7-dimethyl-1-octanethiol.....	27
10.3. Alternative synthesis of 1,4-dithioalkylbenzene 2a using <i>t</i> -BuLi and alkyl bromide	27
10.4. Alternative synthesis of 1,4-dithioalkylbenzene 2e using <i>t</i> -BuLi and alkyl bromide	28
10.5. Alternative synthesis of 1,4-dithioalkylbenzene 2d in DMF	28
10.6. Synthesis of S-PPV monomers 3e and 3a in sealed, pressure resistant vials.....	29
10.7. Synthesis of S-PPV monomer 3a in acetic acid (instead of formic acid)	29
10.8. Synthesis of O-PPV monomers in 1,4-dioxane	30
11. Pictures of polymers 4a and 4b	30
12. Videos of post-polymerization modifications	31
13. References	32

1. Conformational effects

For understanding the expected conformational effects of S-PPVs, it is necessary to take a look at O-PPVs and the (mono)thioalkyl-substituted PPVs reported so far. The optoelectronic properties of O-PPVs are improved by hydrogen bonding between the oxygen atoms and adjacent vinylene hydrogen atoms (Scheme S1 a).^{1,2} The hydrogen bonds lead to reduced torsional twisting, stiffer polymer backbones, and better π -stacking. Furthermore, computational studies revealed that the phenylene units prefer to twist into the same direction, if both hydrogen atoms of the vinylene units can form hydrogen bonds, which requires disubstituted phenylene units.³ As a result, the torsion angles along the polymer backbone have alternating signs, but they have equal (or similar) absolute values, causing a stepped arrangement of the phenylene units in (close-to-)parallel planes. These observations are supported by a single-crystal study of PPV model compounds.⁴ It should be noted that the authors of this study claimed that the distances between the oxygen atoms and adjacent vinylene hydrogen atoms are too large to prove hydrogen bonding. However, the distances in the most accurate model compound (CCDC 113548) are in fact shorter than reported in the text (shorter than 2.4 Å).

Scheme S1. (a) Ideal conformation of O-PPV illustrating the stepped arrangement of the phenylene units in parallel planes, (b) polymer structures of previously reported (mono)thioalkyl-substituted PPVs, (c) PPV with thioalkyl and methoxy substituents illustrating the conformational effect of two different substituents.



For the (mono)thioalkyl-substituted PPVs reported so far (Scheme S1 b),⁵⁻⁷ conformational effects like for O-PPVs and thereby improved optoelectronic properties are unlikely. The polymer with only one substituent at each phenylene unit (Scheme S1 b, top) cannot form hydrogen bonds to both hydrogen atoms of the vinylene units. For the polymer with additional methoxy substituents (Scheme S1 b, bottom), the conformational aspects are more complicated. Both hydrogen atoms of the vinylene units can form hydrogen bonds, and we assume that the phenylene units twist into the same direction. However, the torsion angles will most likely be different depending on the substituent (Scheme S1 c). Considering the reports of increased torsional twisting induced by the larger size of the sulfur atom and taking into account that sulfur is a rather poor hydrogen-bond acceptor,⁸ increased torsion angles are expected for thioalkyl substituents. Consequently, two phenylenes attached to the same vinylene cannot arrange in parallel planes for this polymer, if the polymer is regioregular (only vinylene type **A** is present). If the polymer is not regioregular, some phenylenes attached to the same vinylene can arrange in parallel planes (vinylene types **B** and **C** are present). However, both cases will affect the interchain interactions and the molecular packing, deteriorating the polymer properties.

A comparison of the properties of O-PPVs and the (mono)thioalkyl-substituted PPVs reported so far is not useful, as the preparation methods used for the latter, Wessling route and Heck coupling, yielded polymers with severe defects, which makes a clear assignment of different observations impossible. The Wessling route yielded polymers with a vast number of non-conjugated defects as only 60-70% of the expected vinylenes were formed (due to incomplete elimination).^{5,6} The Heck coupling also yielded polymers with many structural defects, as indicated by the complex ¹H NMR spectra.⁷ Insolubility, low (or not given) reaction yields, and low molecular weights are additional issues of these polymers. Except for two small studies of OLEDs and cathodoluminescence,^{9,10} no further investigations of these polymers were reported.

In contrast to the (mono)thioalkyl-substituted PPVs, S-PPVs are expected to show conformational effects like O-PPVs, as two substituents of the same kind are present at each phenylene unit. Increased torsion angles are expected to alter the step height between the phenylene units, but not their arrangement in parallel planes. The torsions induced by the larger size of the sulfur atom balance out, which is in sharp contrast to other thioalkyl-substituted conjugated polymers. Of course, increased step height can still result in reduced effective conjugation length, but we expected that the positive effects of intermolecular S...S interactions and lower HOMO and LUMO energy levels on the material properties prevail.

2. ^1H and ^{13}C (APT) NMR spectra

NMR spectra were recorded at 600 MHz for ^1H and 151 MHz for ^{13}C on a Bruker Avance III HD spectrometer. For ^{13}C NMR signals, the number of attached protons (C, CH, CH_2 , CH_3) was assigned by attached proton test (APT) experiments.

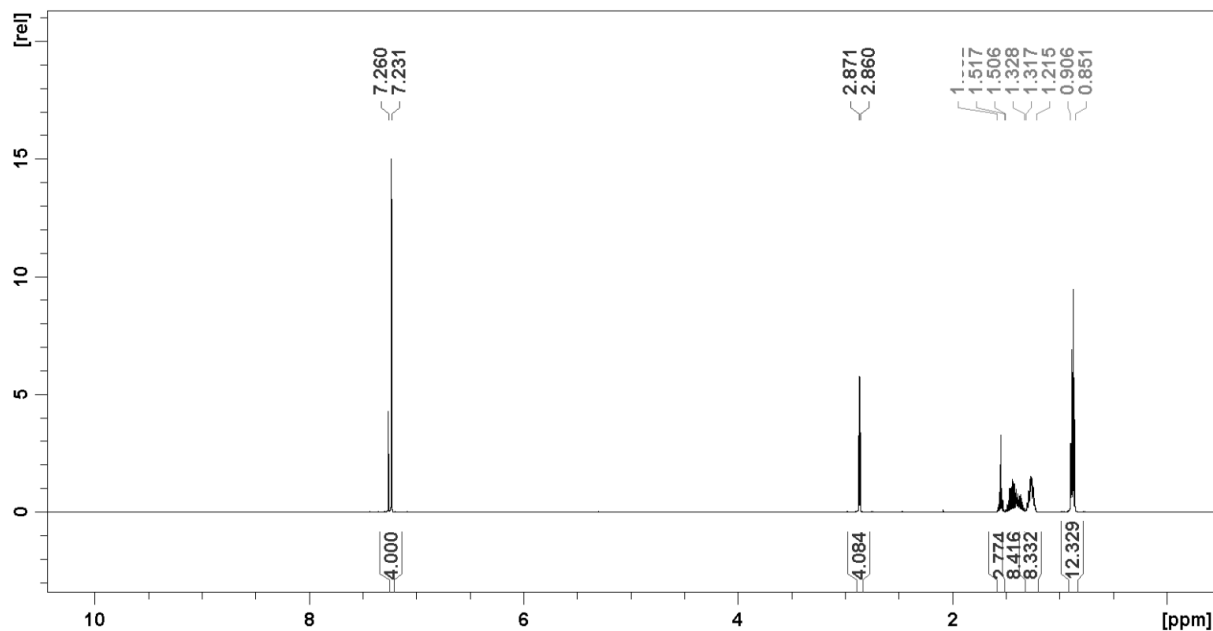


Figure S1: ^1H NMR spectrum (600 MHz, CDCl_3) of 2a.

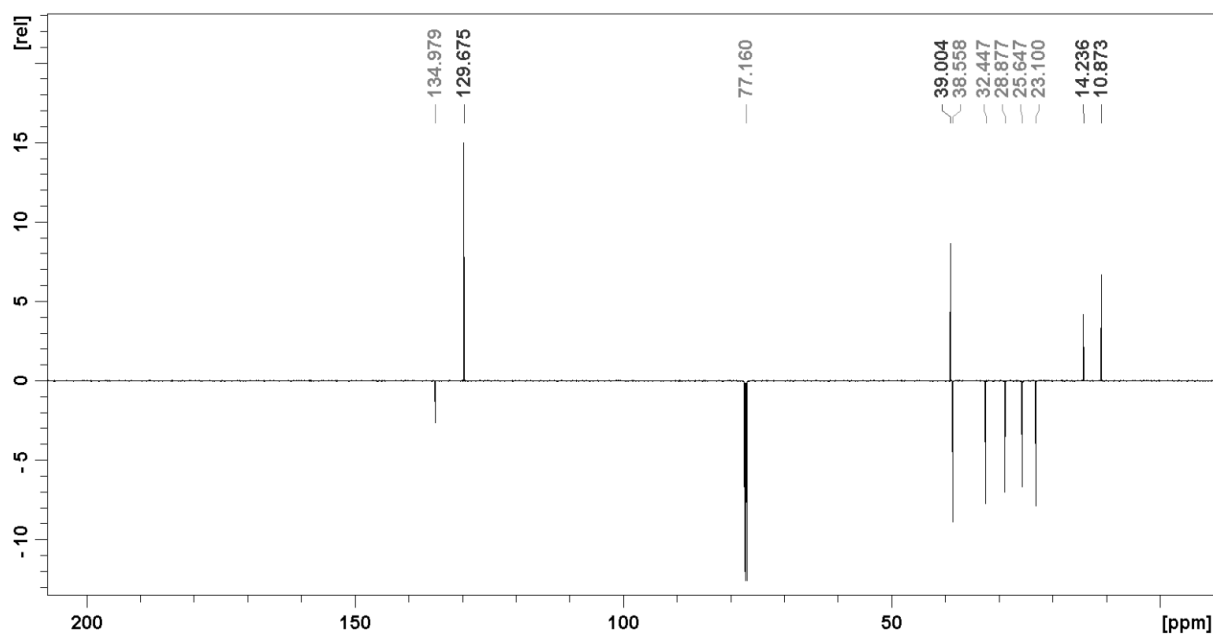


Figure S2: ^{13}C (APT) NMR spectrum (150 MHz, CDCl_3) of 2a.

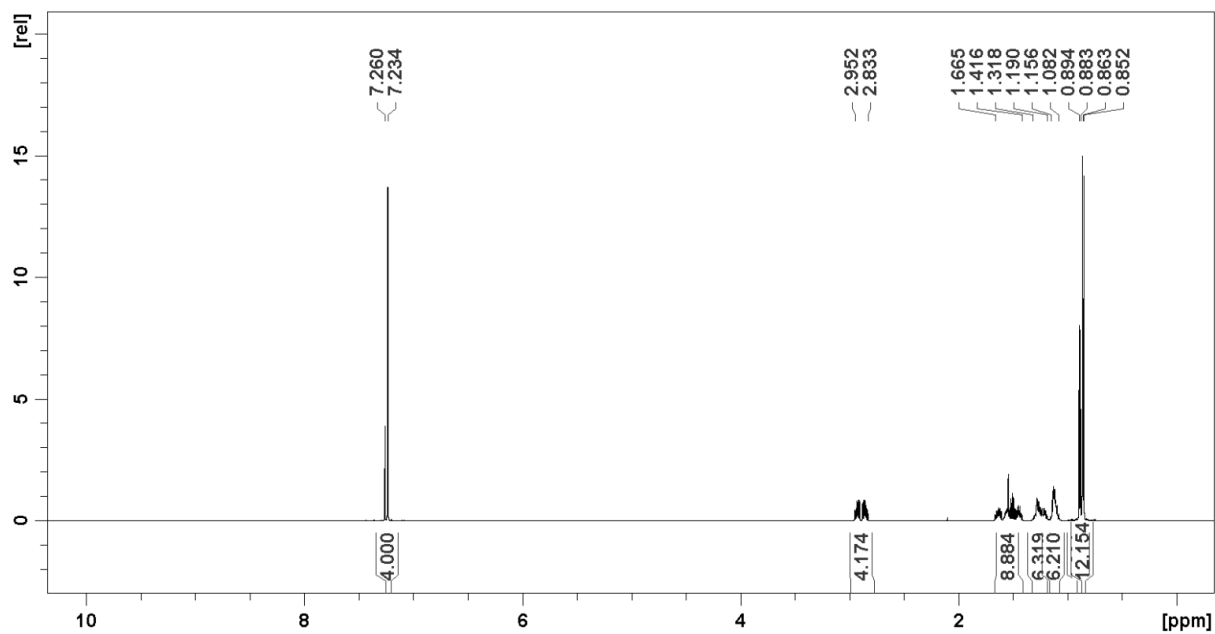


Figure S3: ^1H NMR spectrum (600 MHz, CDCl_3) of **2b**.

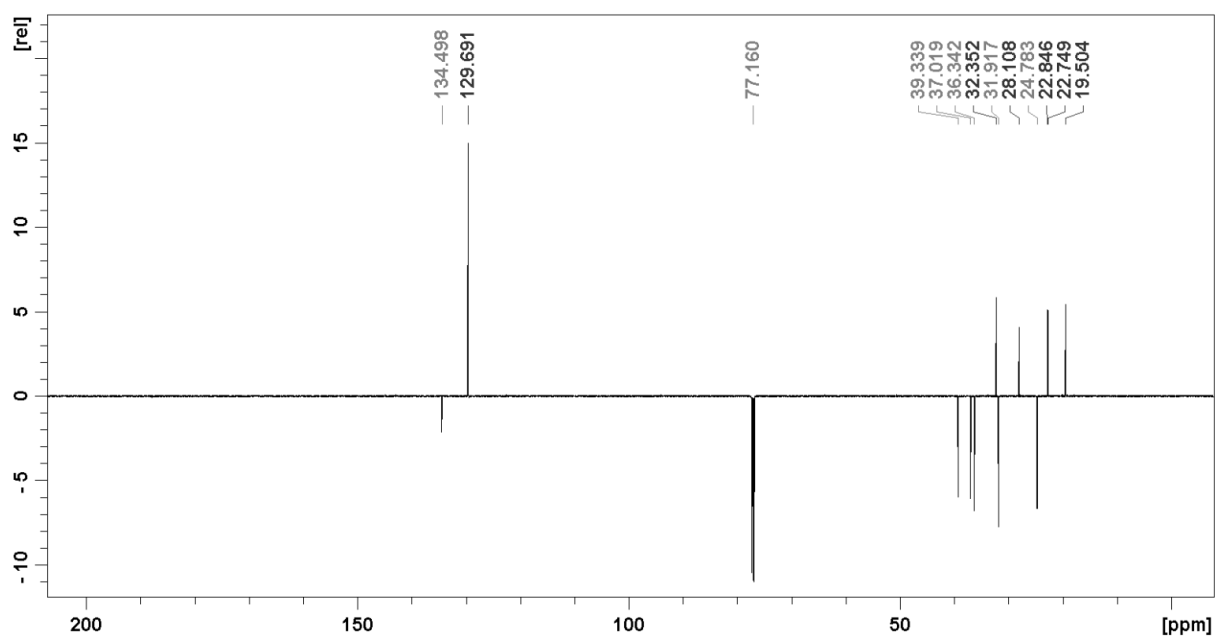


Figure S4: ^{13}C (APT) NMR spectrum (150 MHz, CDCl_3) of **2b**.

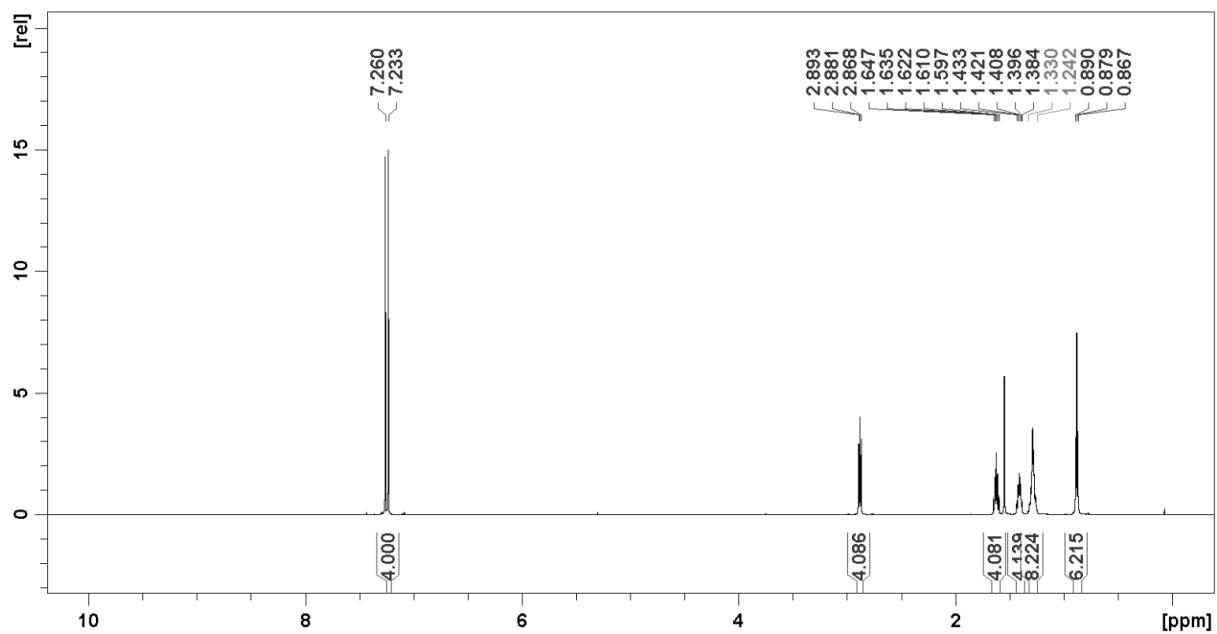


Figure S5: ^1H NMR spectrum (600 MHz, CDCl_3) of **2c**.

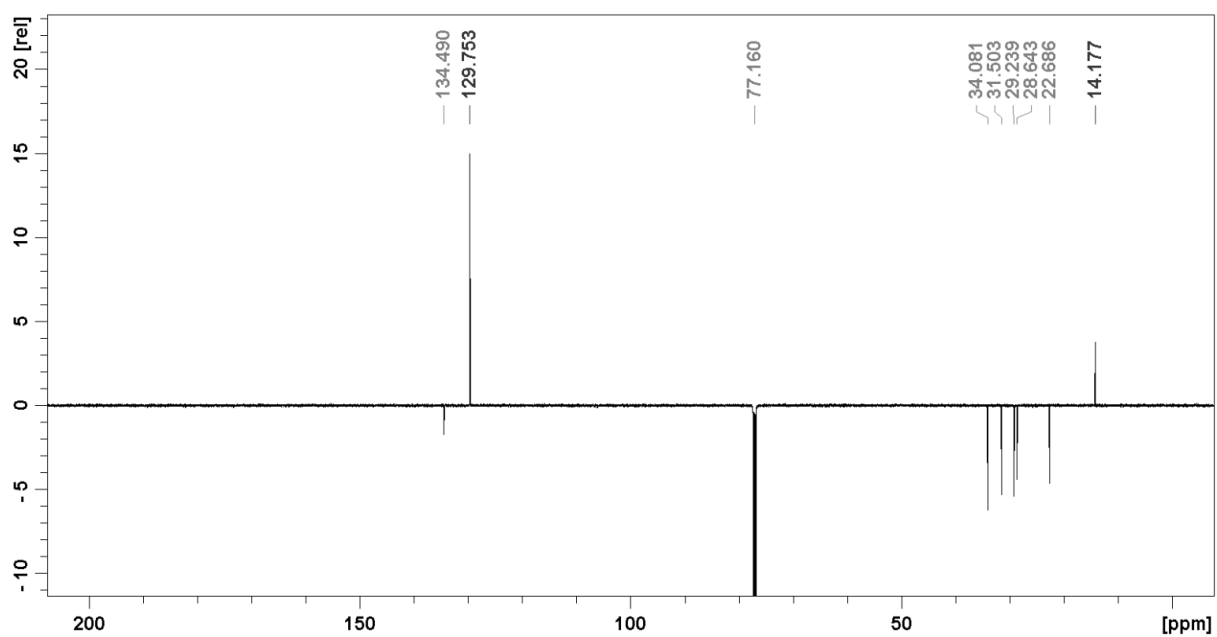


Figure S6: ^{13}C (APT) NMR spectrum (150 MHz, CDCl_3) of **2c**.

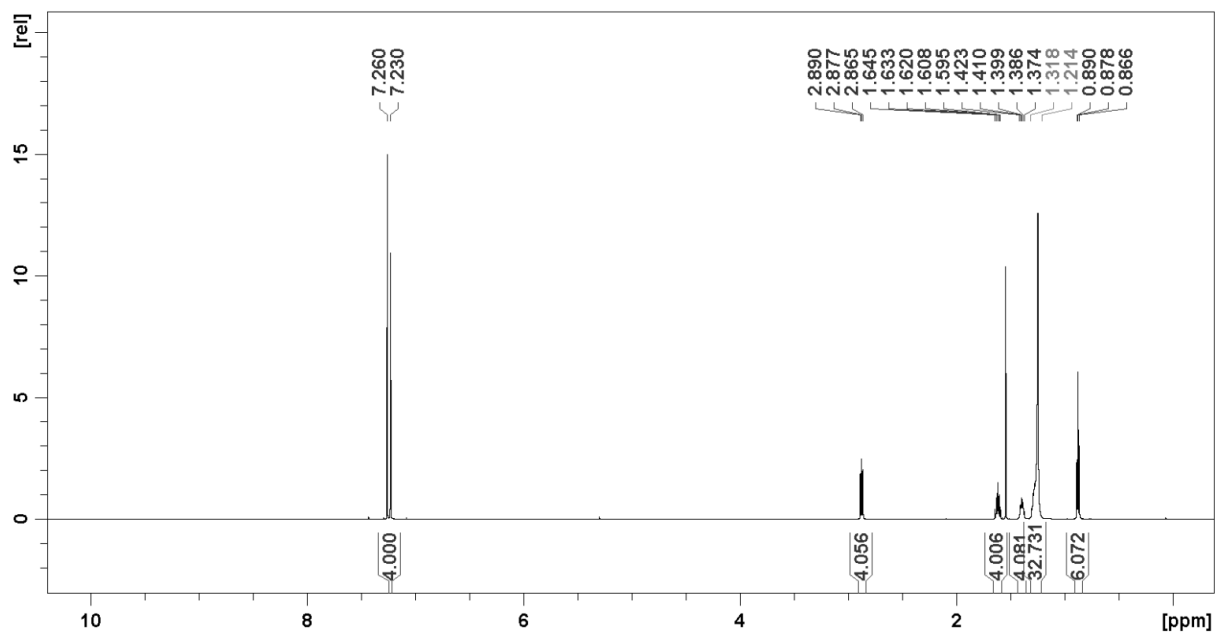


Figure S7: ^1H NMR spectrum (600 MHz, CDCl_3) of **2d**.

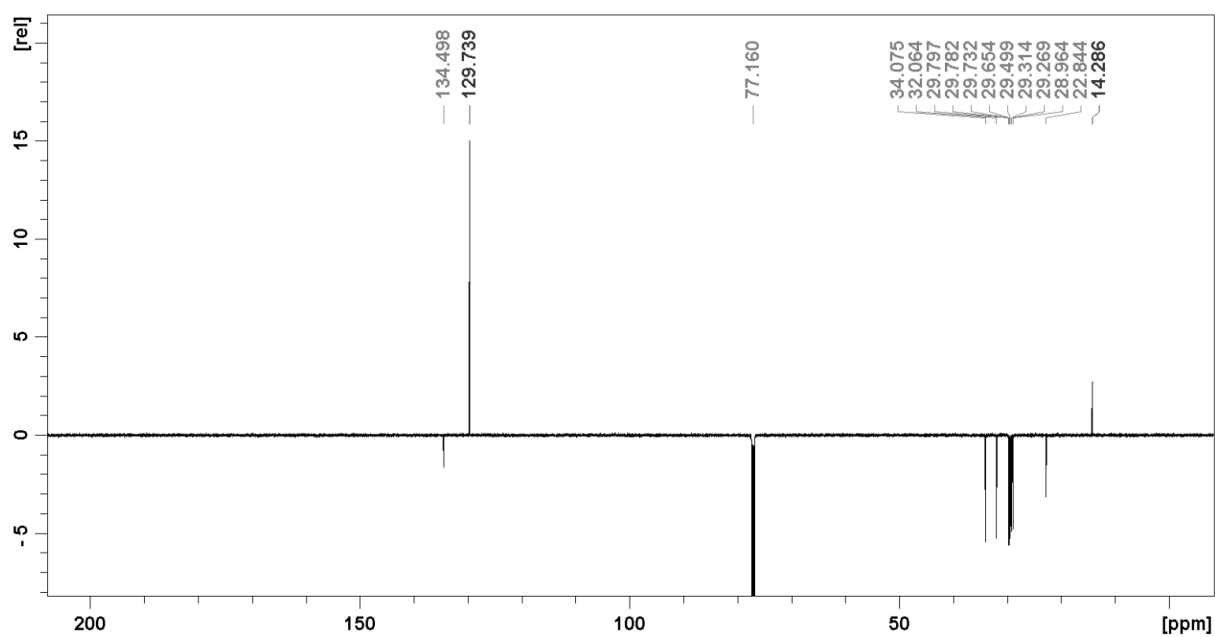


Figure S8: ^{13}C (APT) NMR spectrum (150 MHz, CDCl_3) of **2d**.

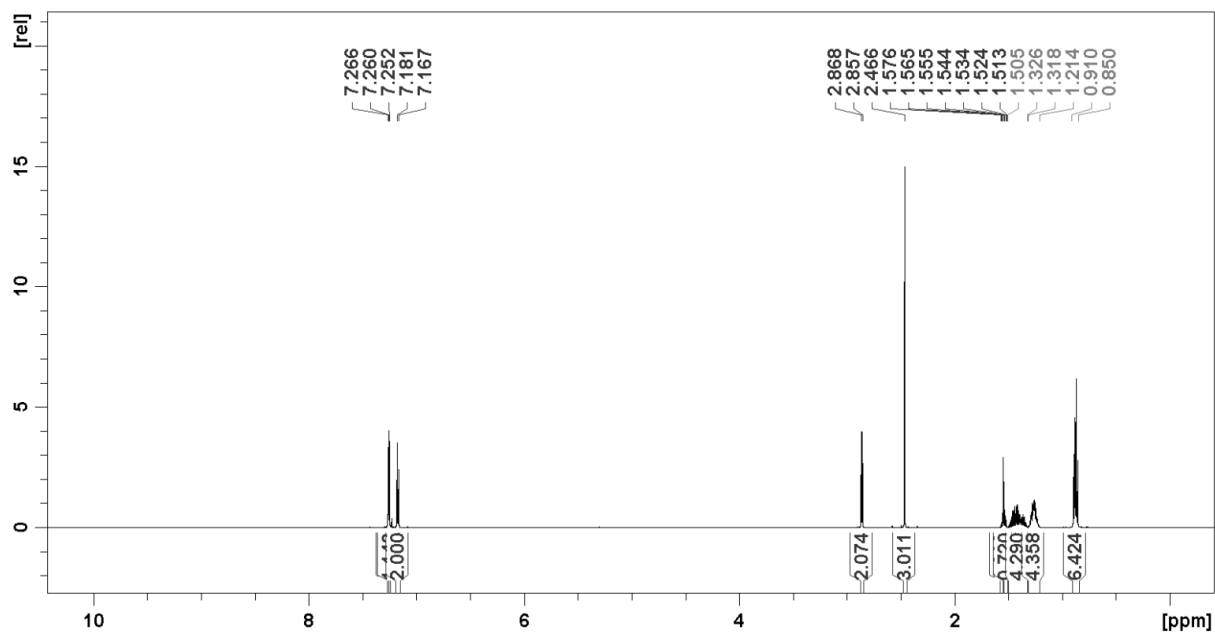


Figure S9: ^1H NMR spectrum (600 MHz, CDCl_3) of **2e**.

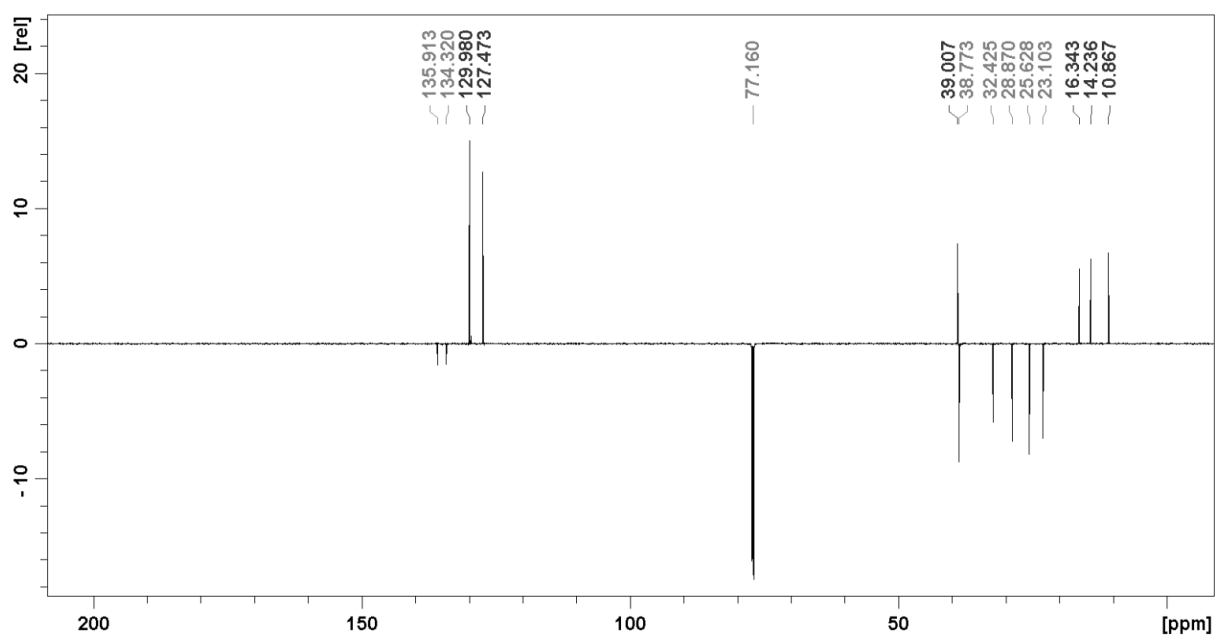


Figure S10: ^{13}C (APT) NMR spectrum (150 MHz, CDCl_3) of **2e**.

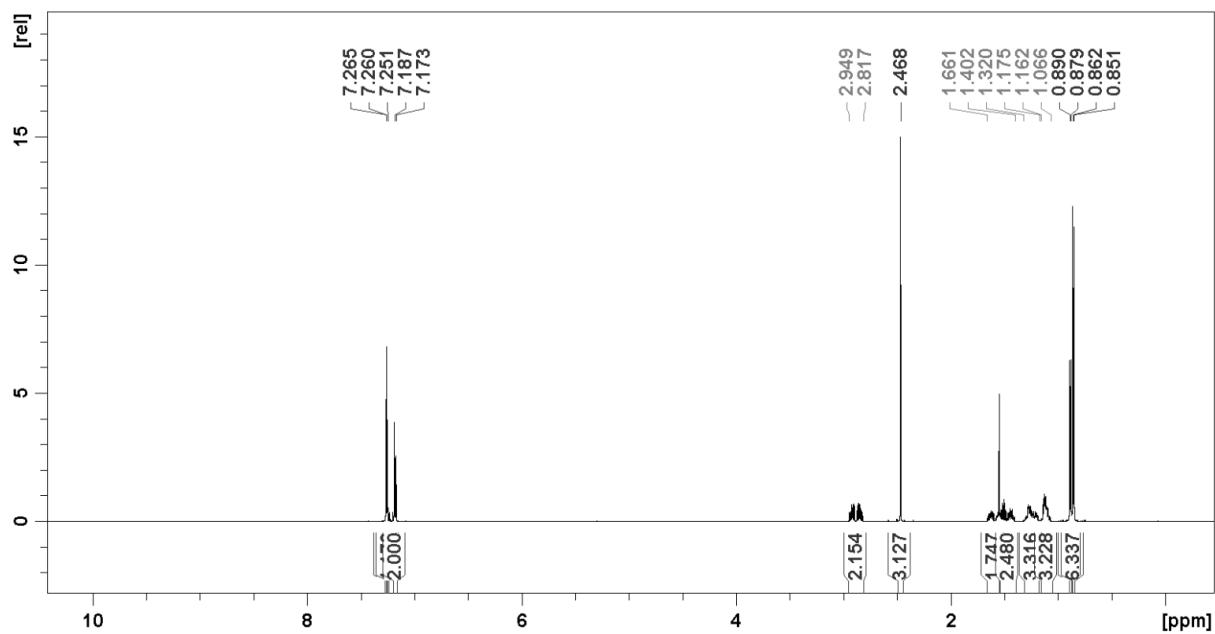


Figure S11: ^1H NMR spectrum (600 MHz, CDCl_3) of **2f**.

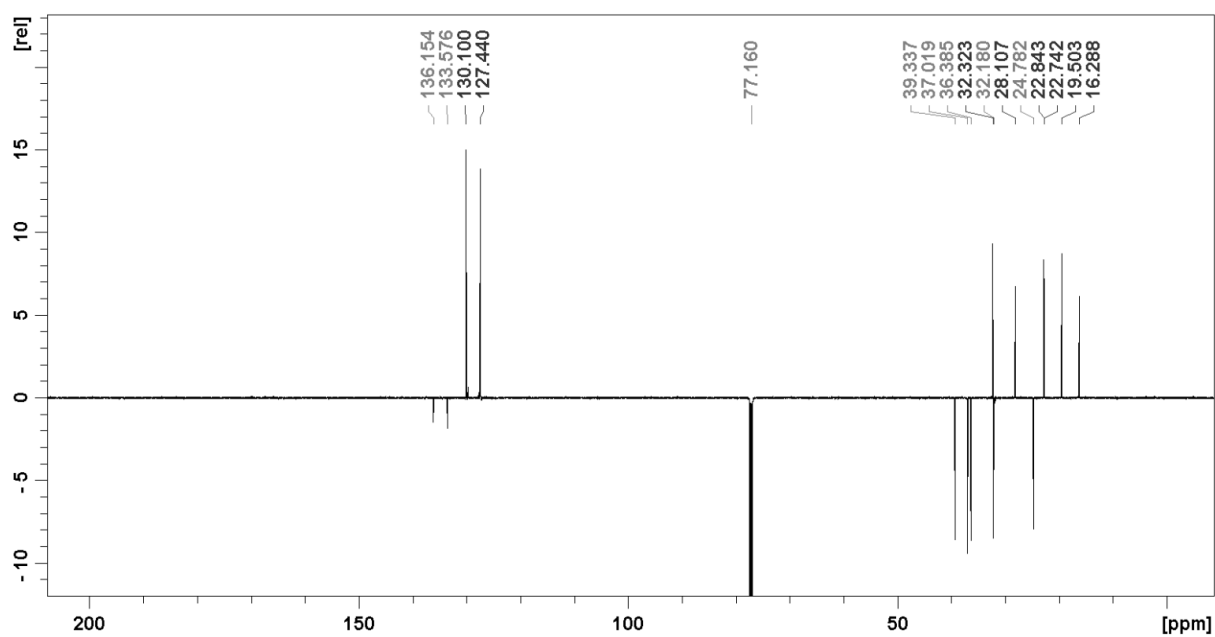


Figure S12: ^{13}C (APT) NMR spectrum (150 MHz, CDCl_3) of **2f**.

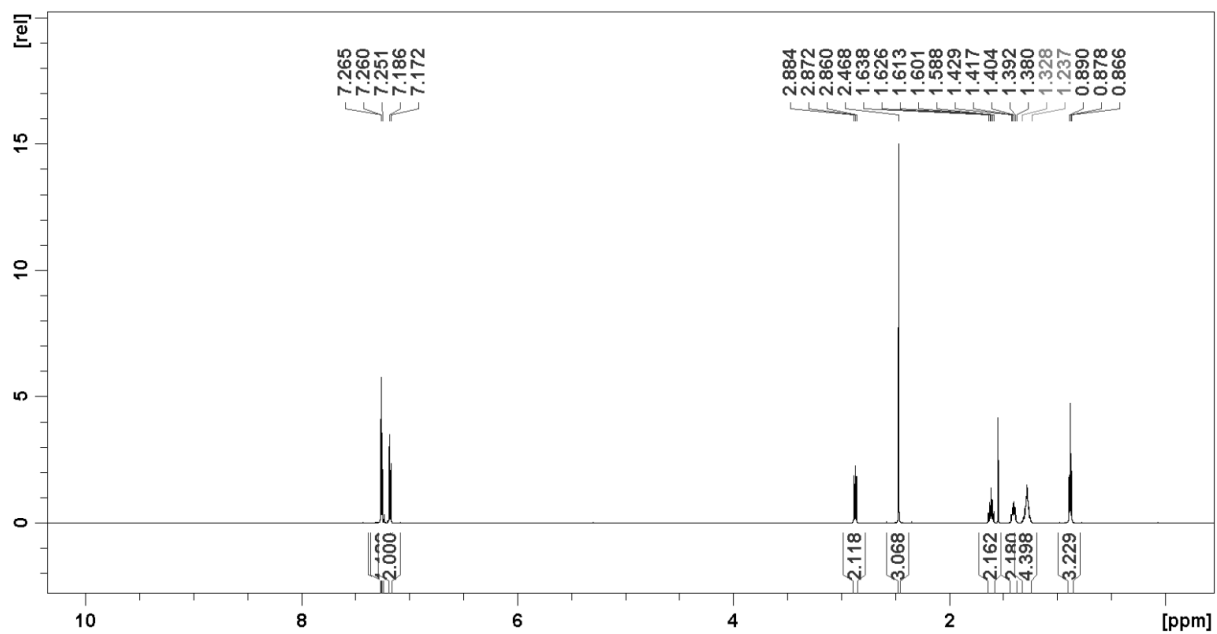


Figure S13: ^1H NMR spectrum (600 MHz, CDCl_3) of **2g**.

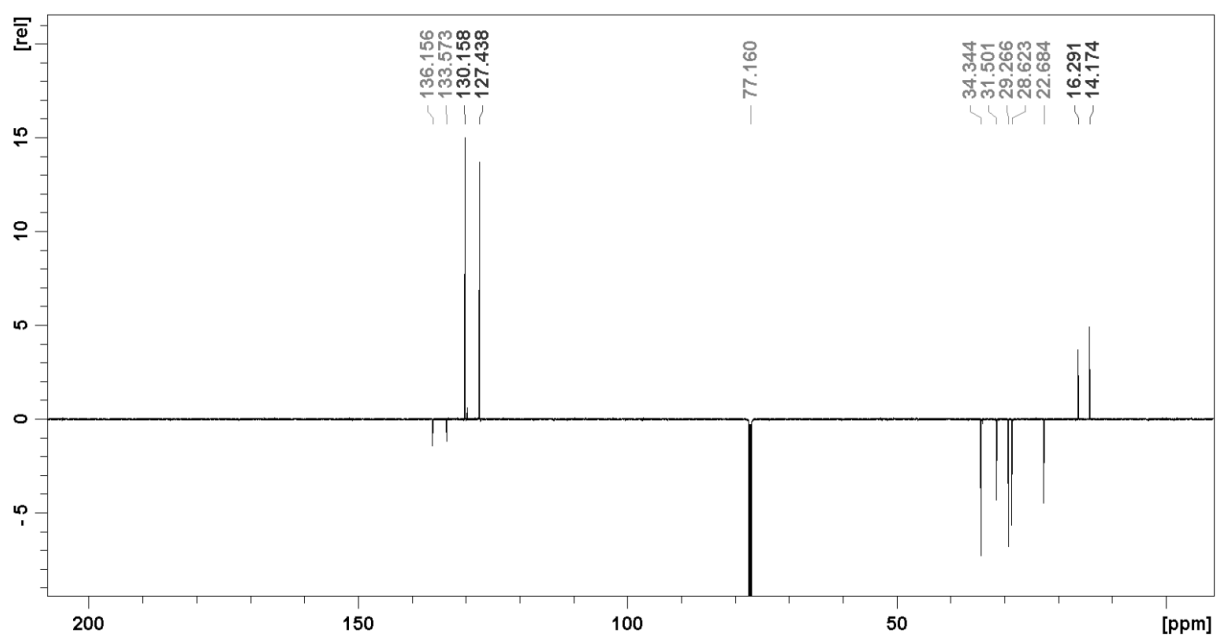


Figure S14: ^{13}C (APT) NMR spectrum (150 MHz, CDCl_3) of **2g**.

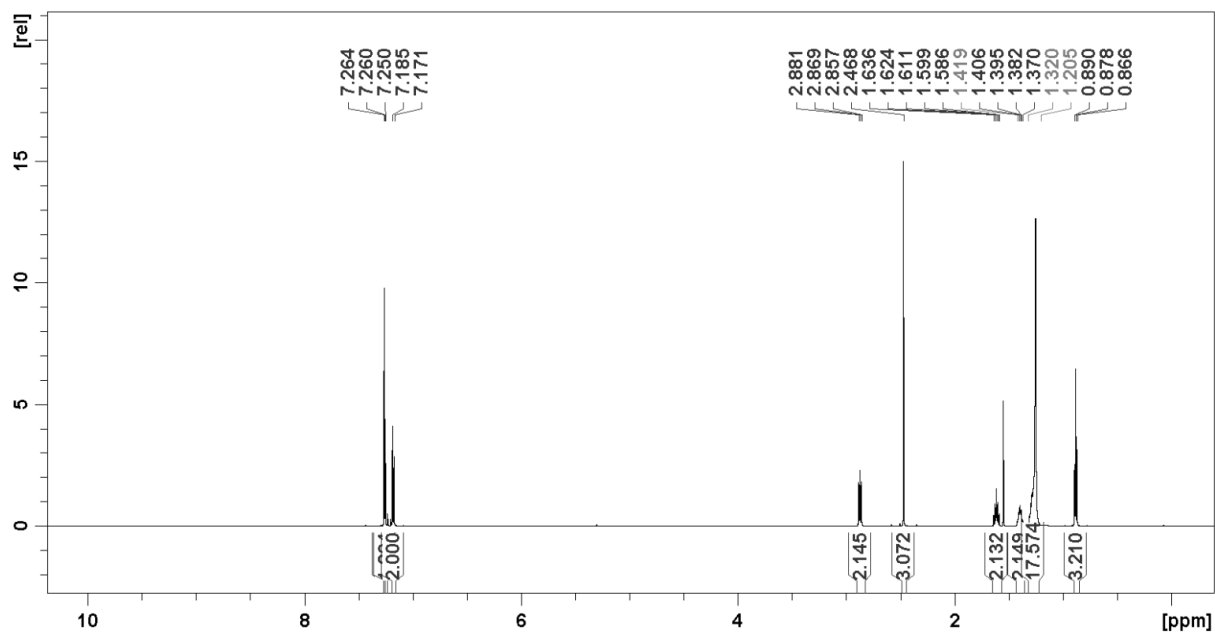


Figure S15: ^1H NMR spectrum (600 MHz, CDCl_3) of **2h**.

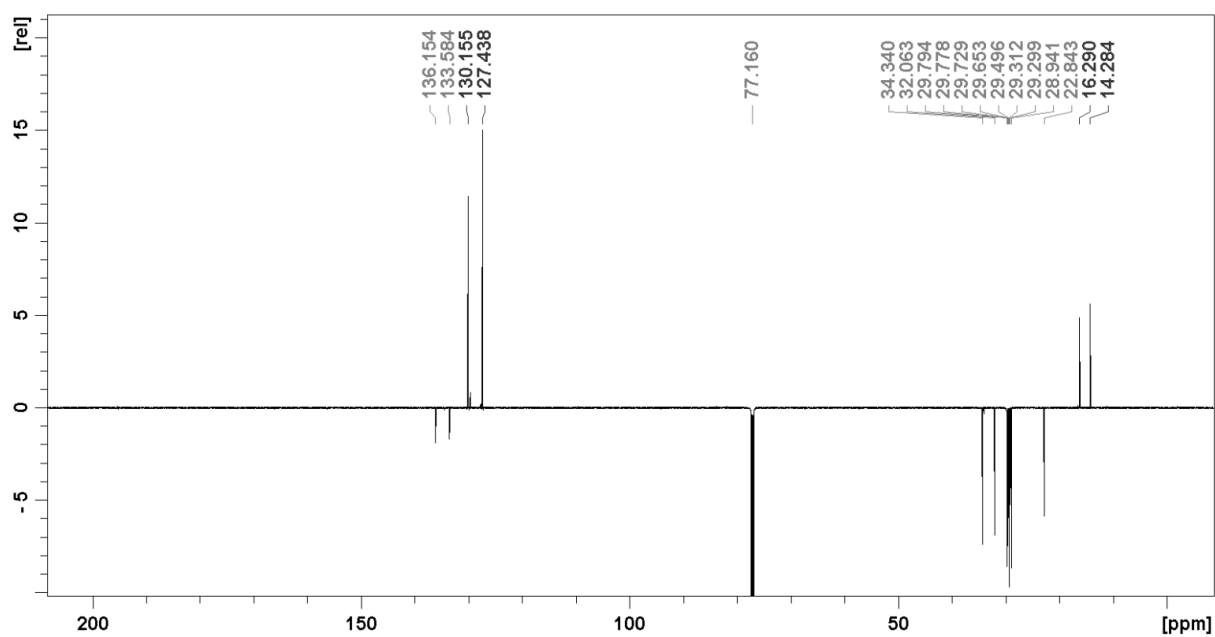


Figure S16: ^{13}C (APT) NMR spectrum (150 MHz, CDCl_3) of **2h**.

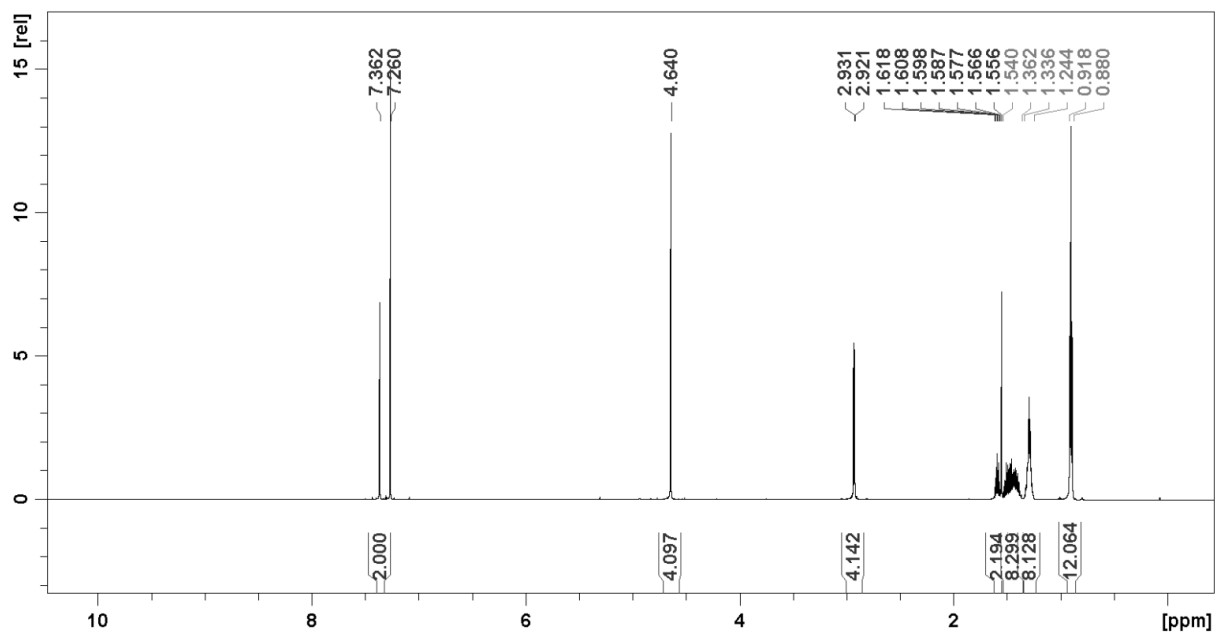


Figure S17: ^1H NMR spectrum (600 MHz, CDCl_3) of **3a**.

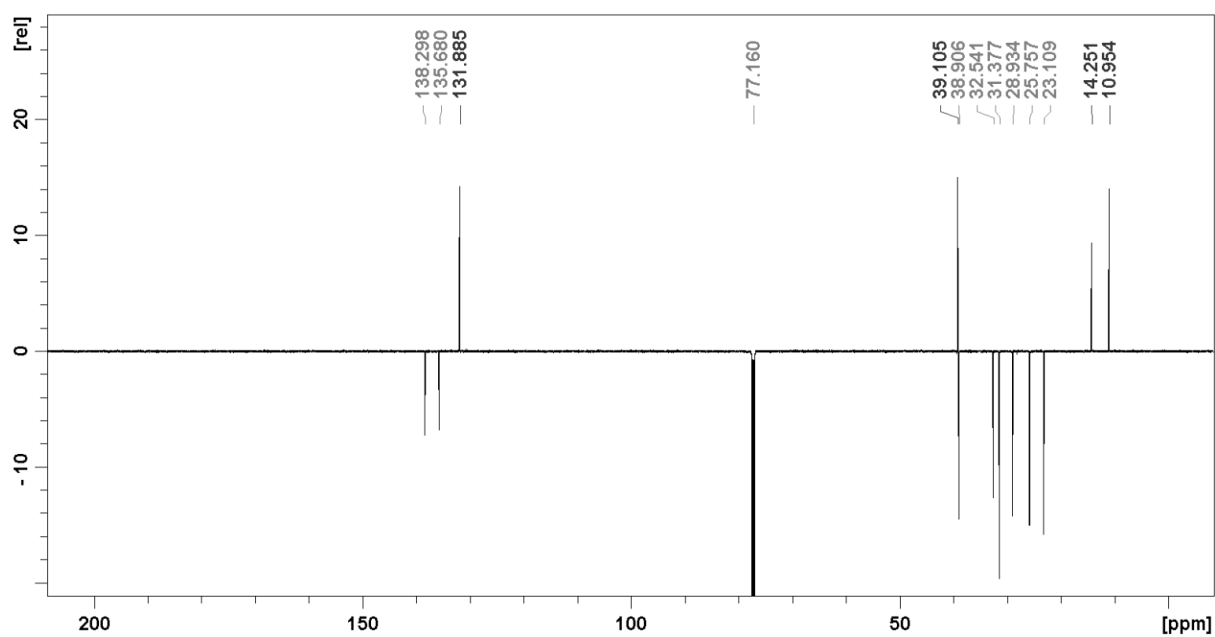


Figure S18: ^{13}C (APT) NMR spectrum (150 MHz, CDCl_3) of **3a**.

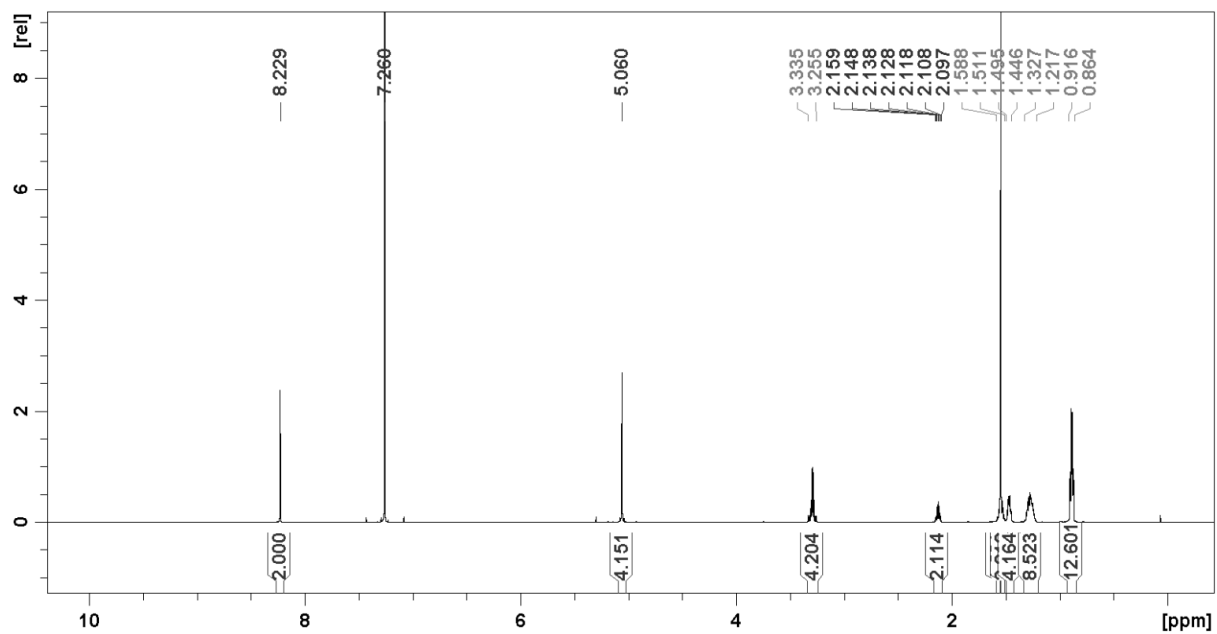


Figure S19: ^1H NMR spectrum (600 MHz, CDCl_3) of **3a-SO₂**.

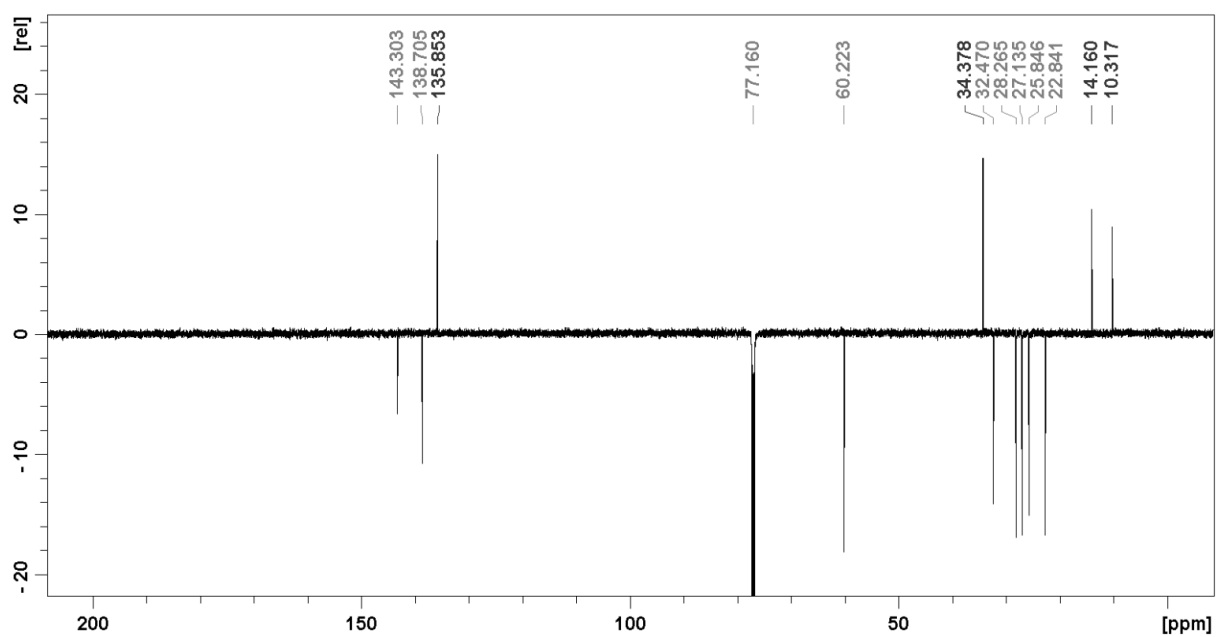


Figure S20: ^{13}C (APT) NMR spectrum (150 MHz, CDCl_3) of **3a-SO₂**.

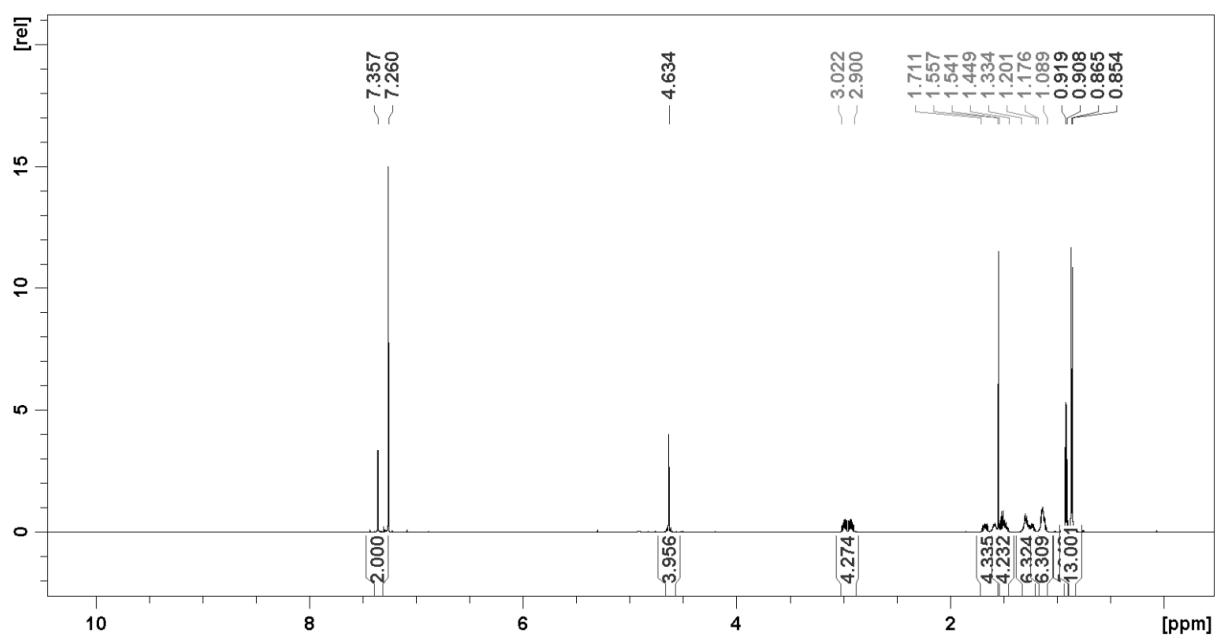


Figure S21: ^1H NMR spectrum (600 MHz, CDCl_3) of **3b**.

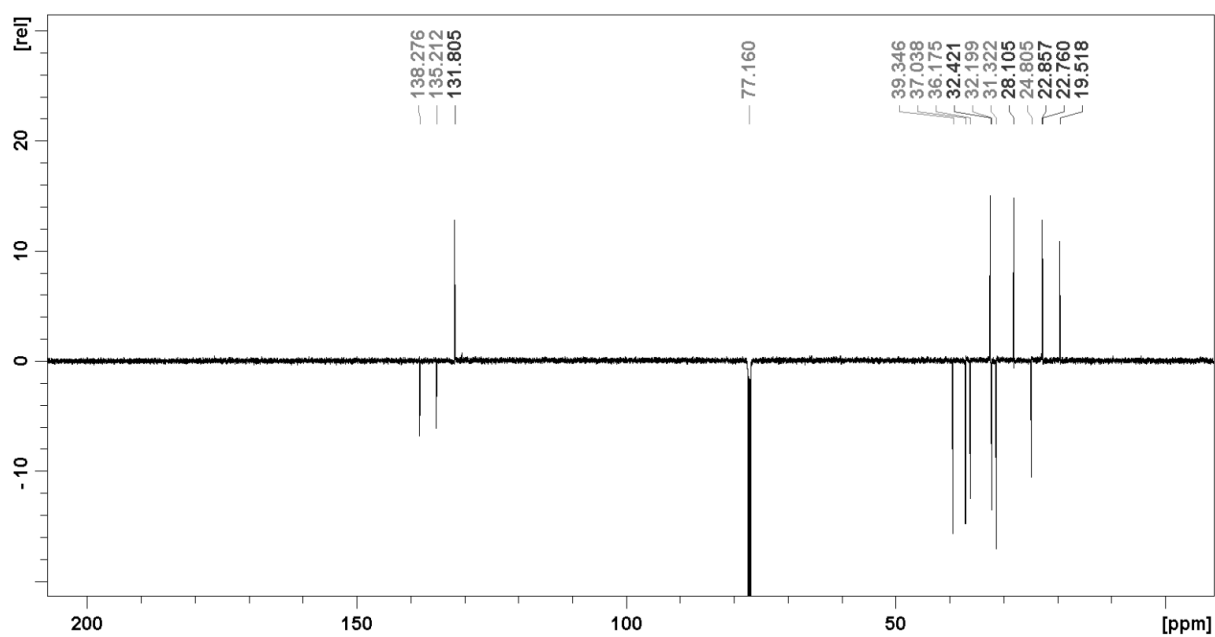


Figure S22: ^{13}C (APT) NMR spectrum (150 MHz, CDCl_3) of **3b**.

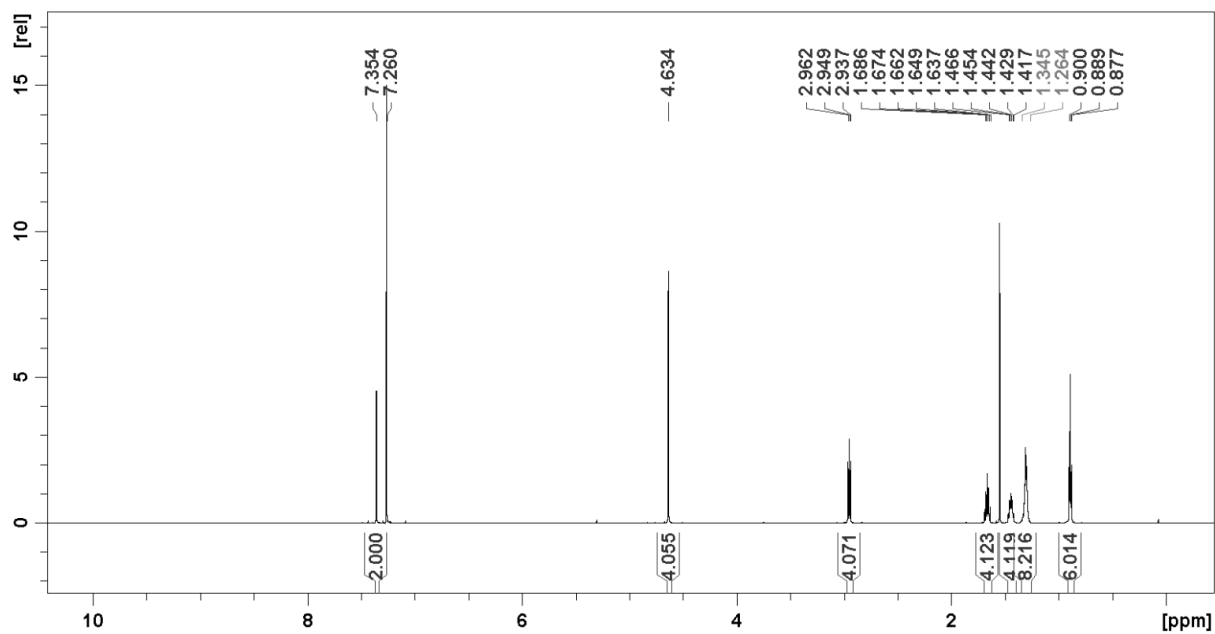


Figure S23: ^1H NMR spectrum (600 MHz, CDCl_3) of **3c**.

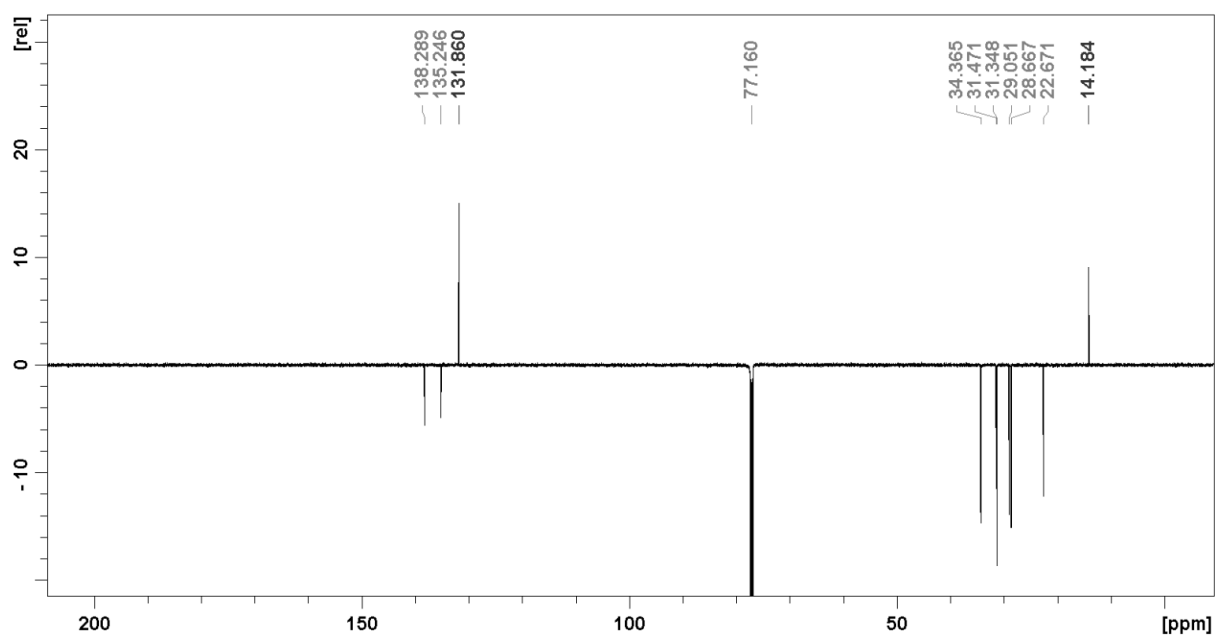


Figure S24: ^{13}C (APT) NMR spectrum (150 MHz, CDCl_3) of **3c**.

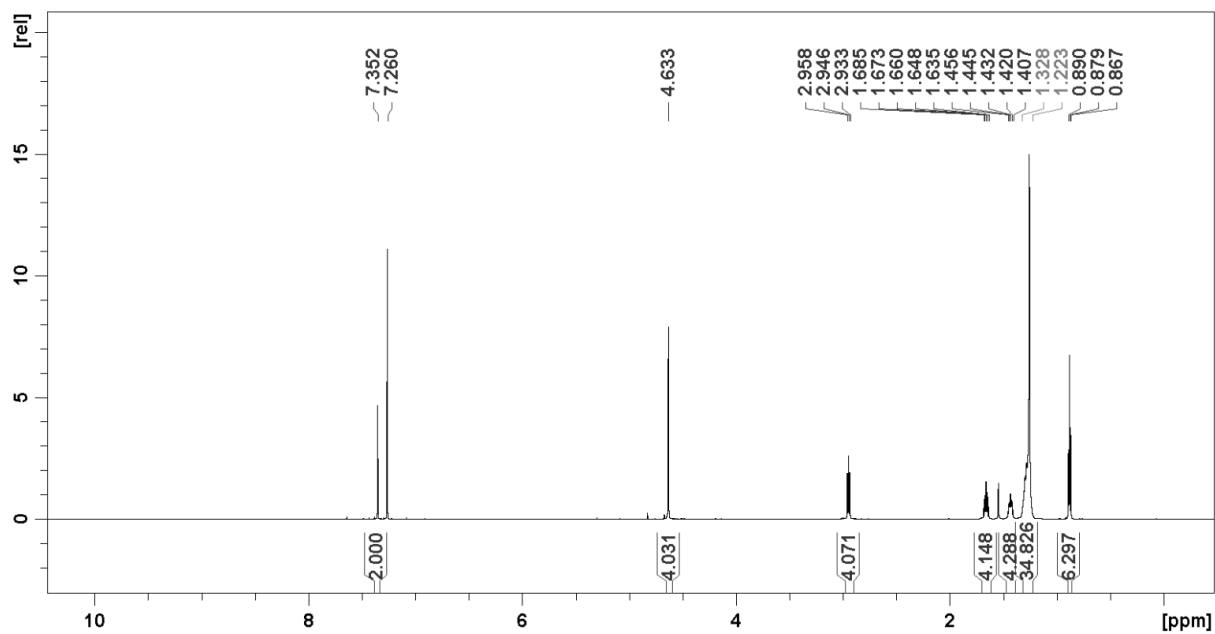


Figure S25: ^1H NMR spectrum (600 MHz, CDCl_3) of **3d**.

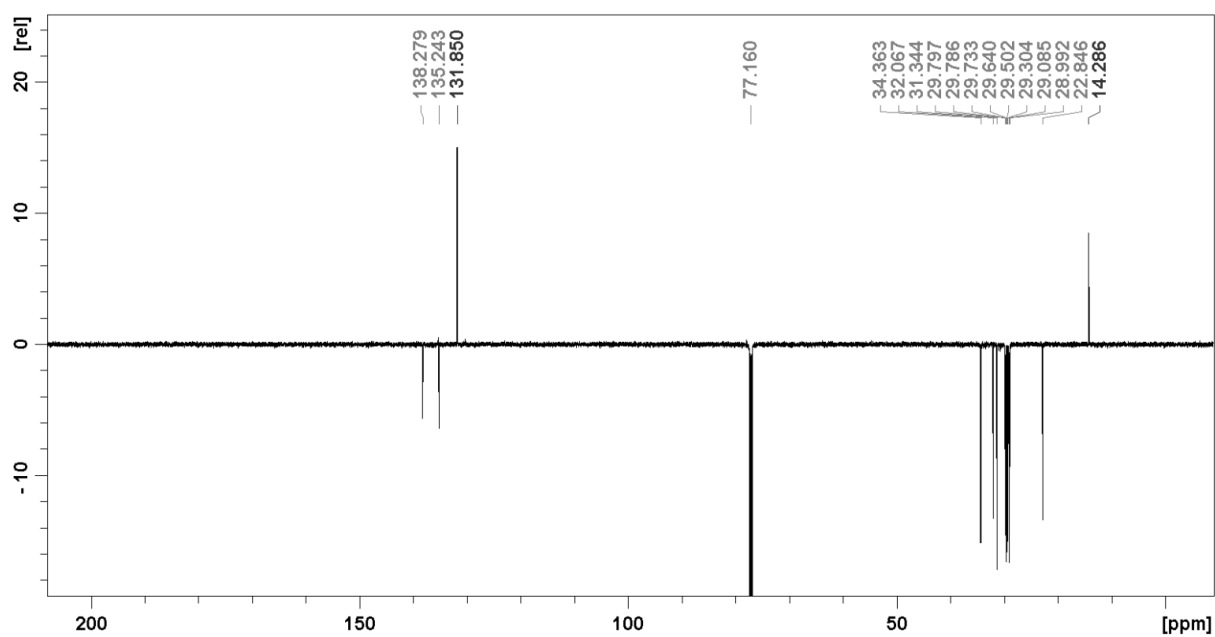


Figure S26: ^{13}C (APT) NMR spectrum (150 MHz, CDCl_3) of **3d**.

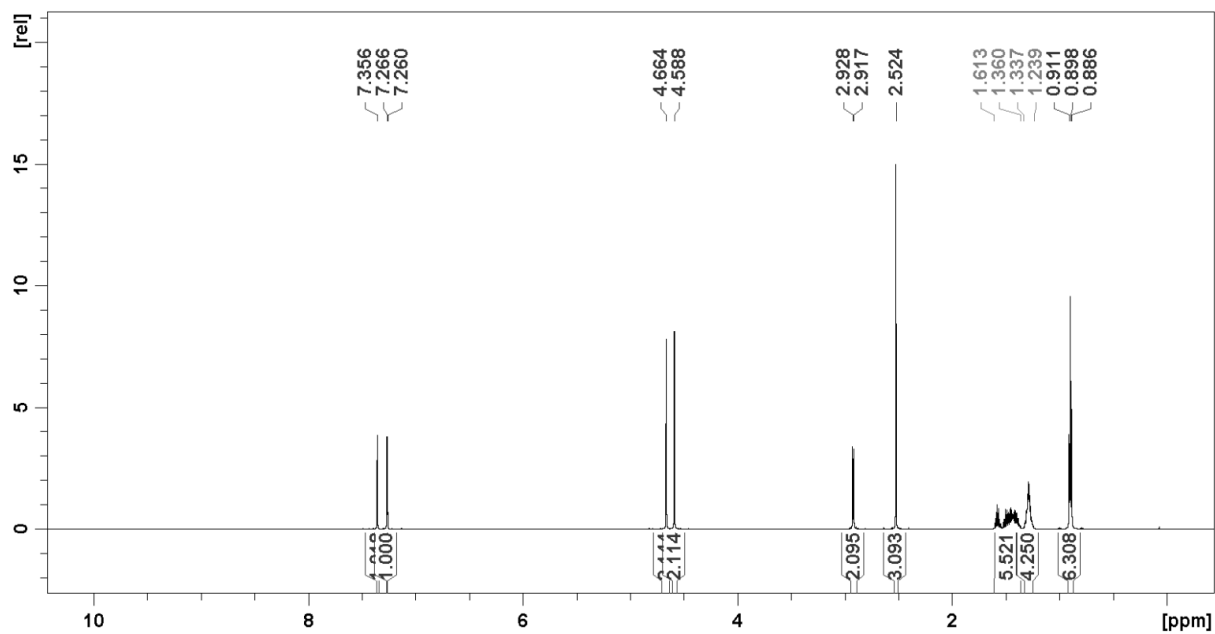


Figure S27: ¹H NMR spectrum (600 MHz, CDCl₃) of **3e**.

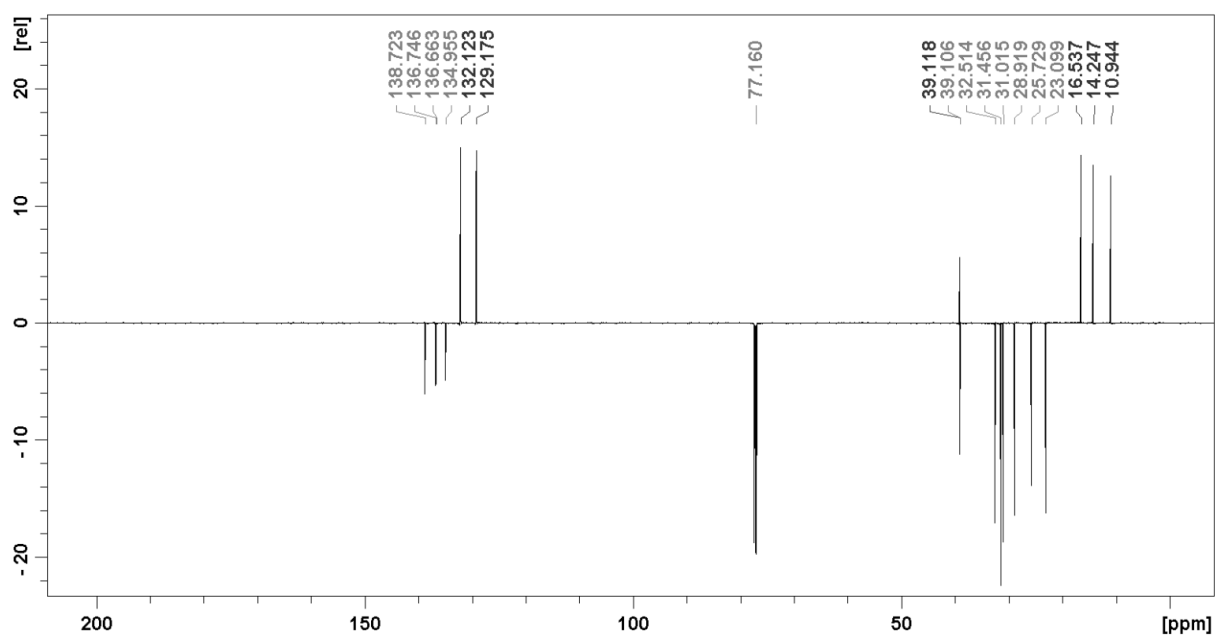


Figure S28: ¹³C(APT) NMR spectrum (150 MHz, CDCl₃) of **3e**.

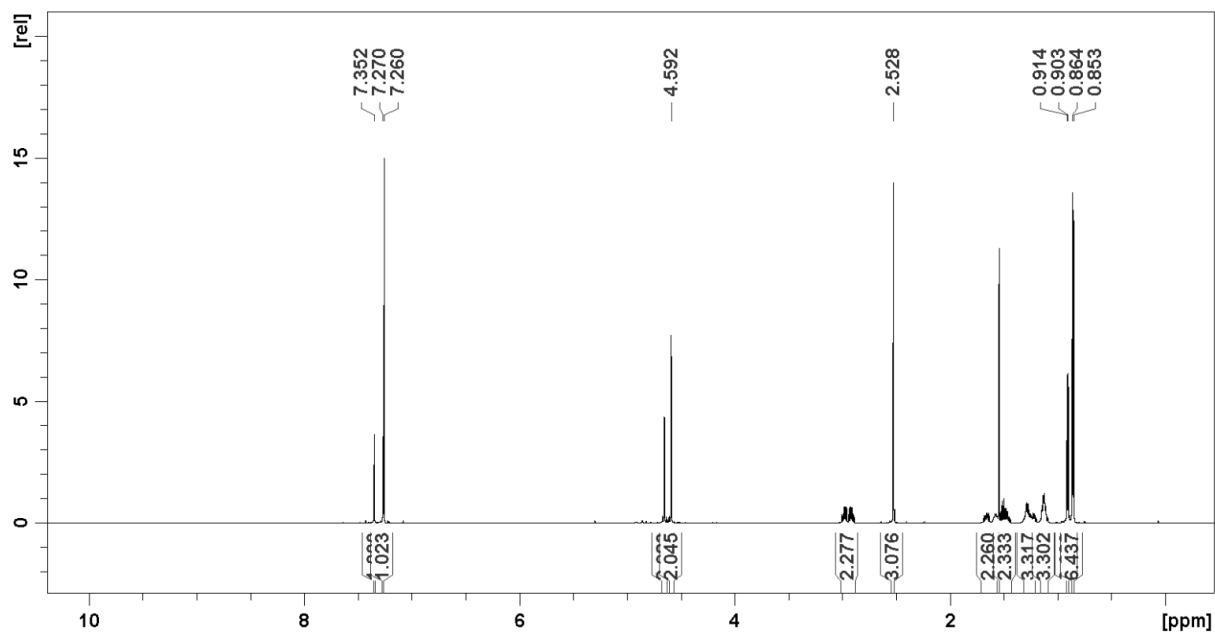


Figure S29: ¹H NMR spectrum (600 MHz, CDCl₃) of 3f.

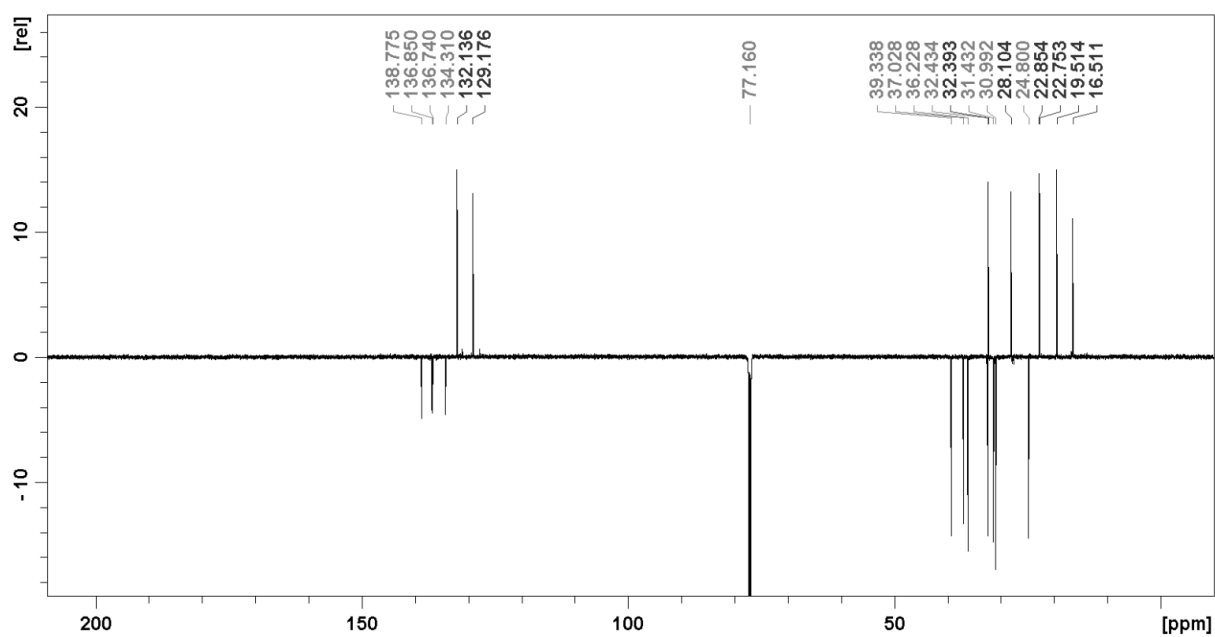


Figure S30: ¹³C(APT) NMR spectrum (150 MHz, CDCl₃) of 3f.

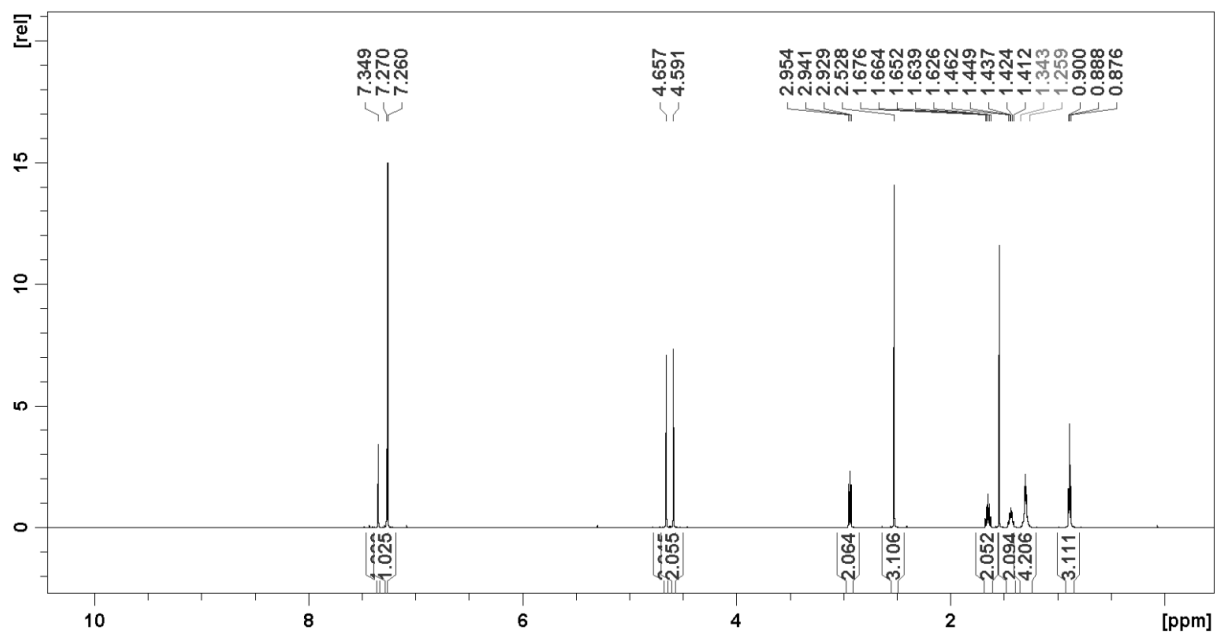


Figure S31: ^1H NMR spectrum (600 MHz, CDCl_3) of **3g**.

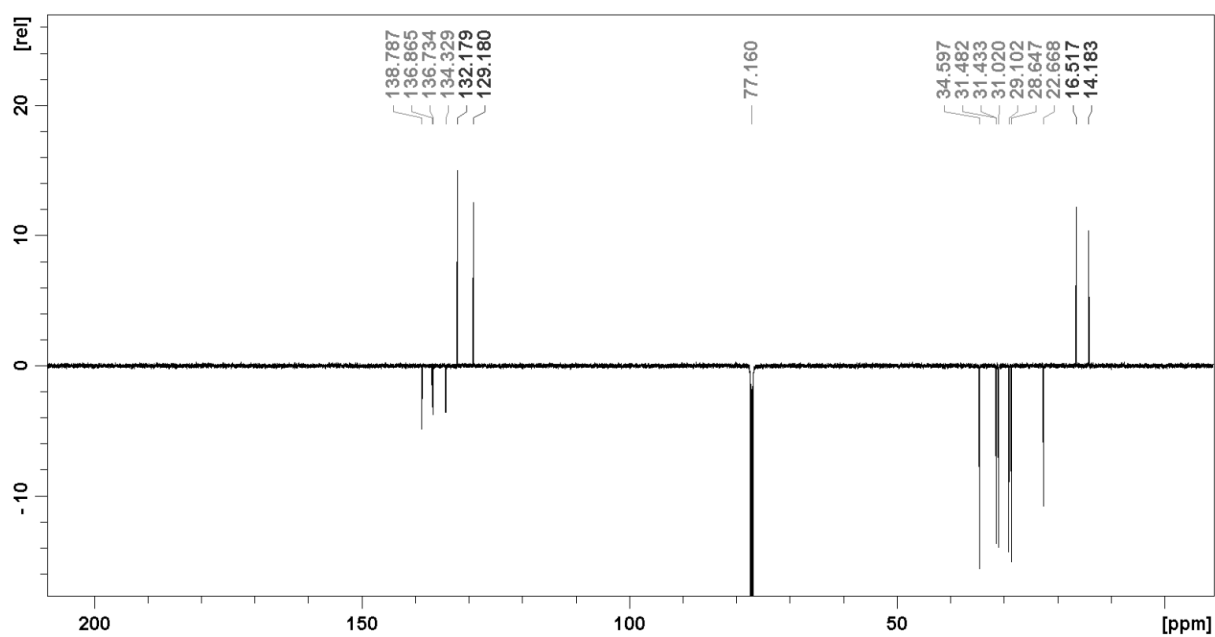


Figure S32: ^{13}C (APT) NMR spectrum (150 MHz, CDCl_3) of **3g**.

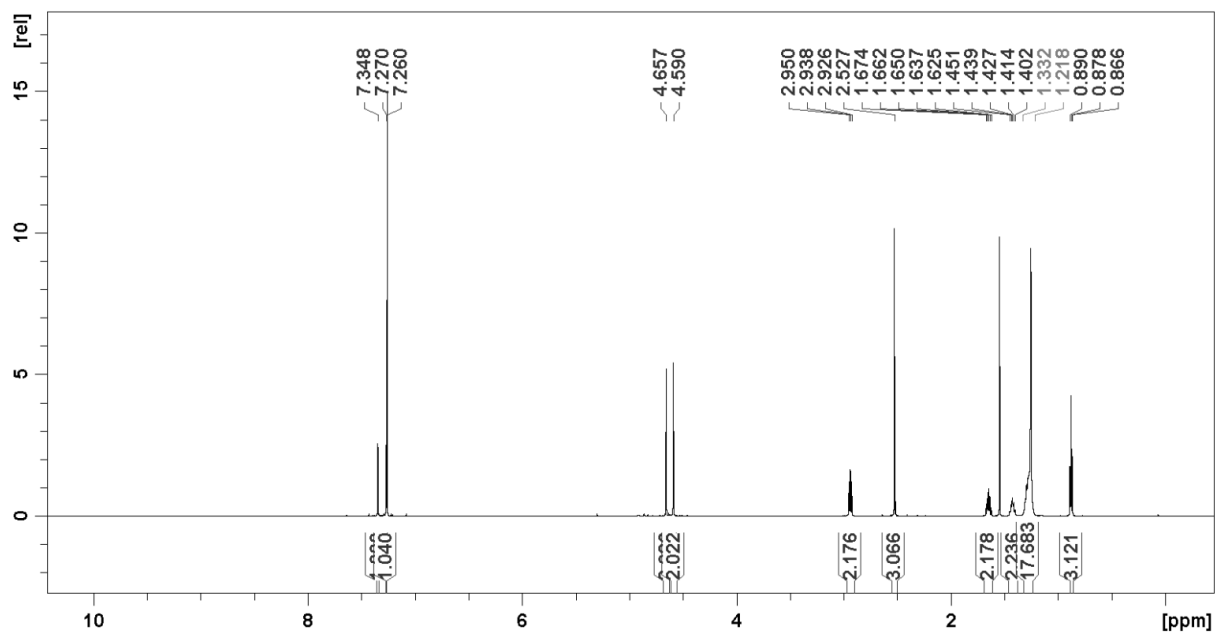


Figure S33: ^1H NMR spectrum (600 MHz, CDCl_3) of **3h**.

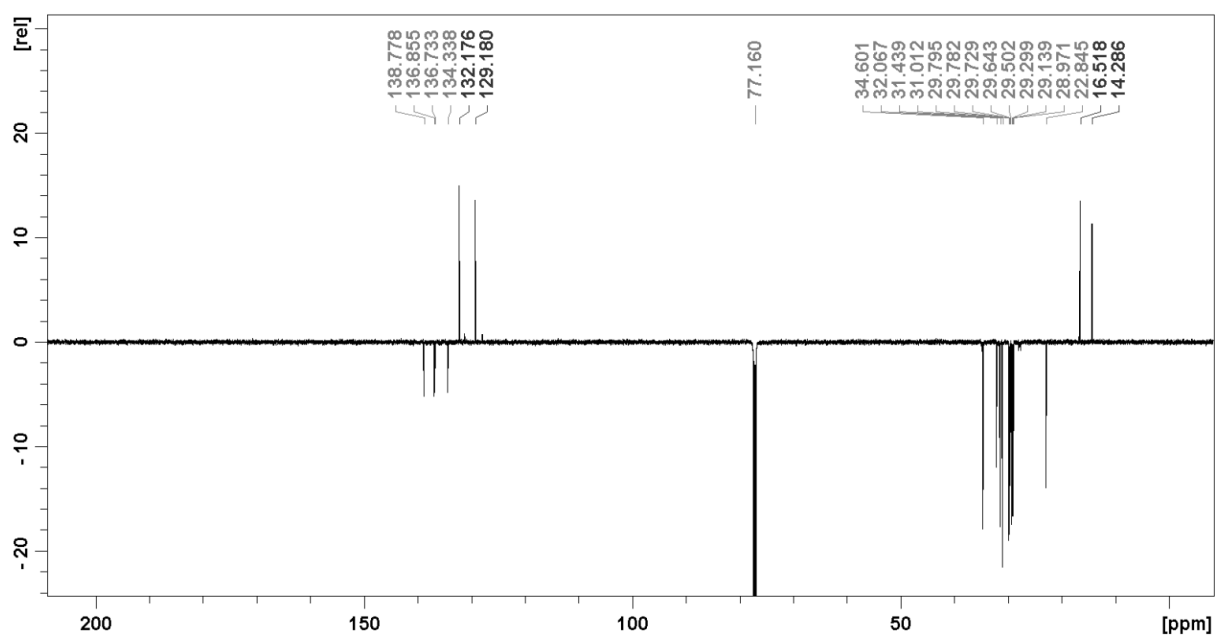


Figure S34: ^{13}C (APT) NMR spectrum (150 MHz, CDCl_3) of **3h**.

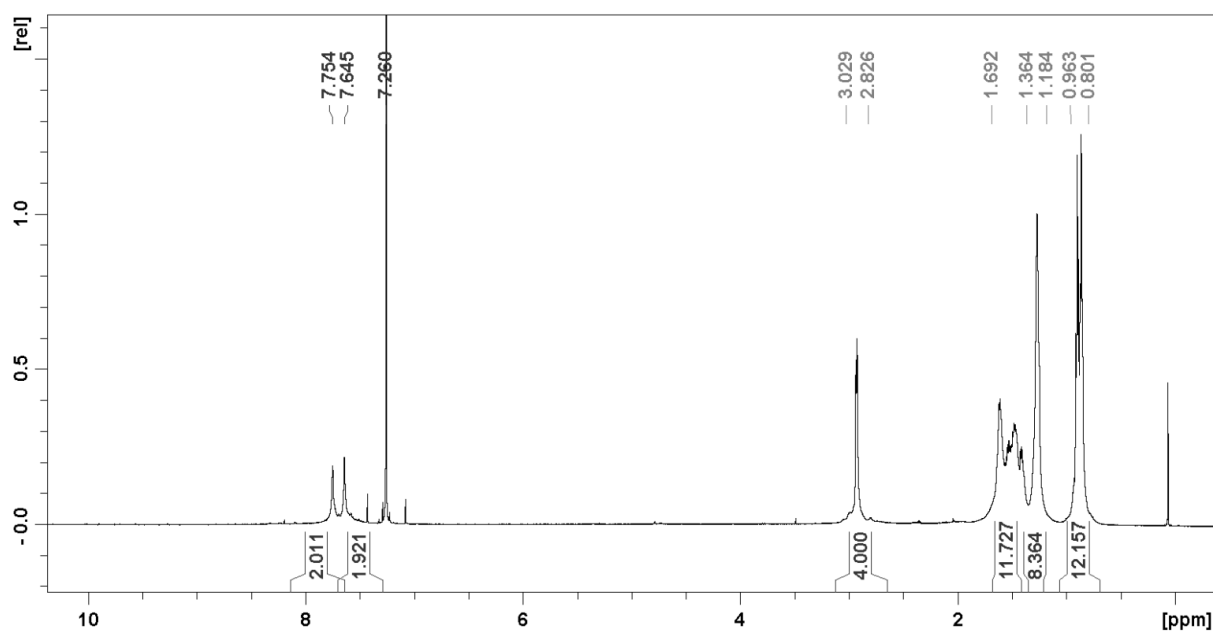


Figure S35: ^1H NMR spectrum (600 MHz, CDCl_3) of **4a**.

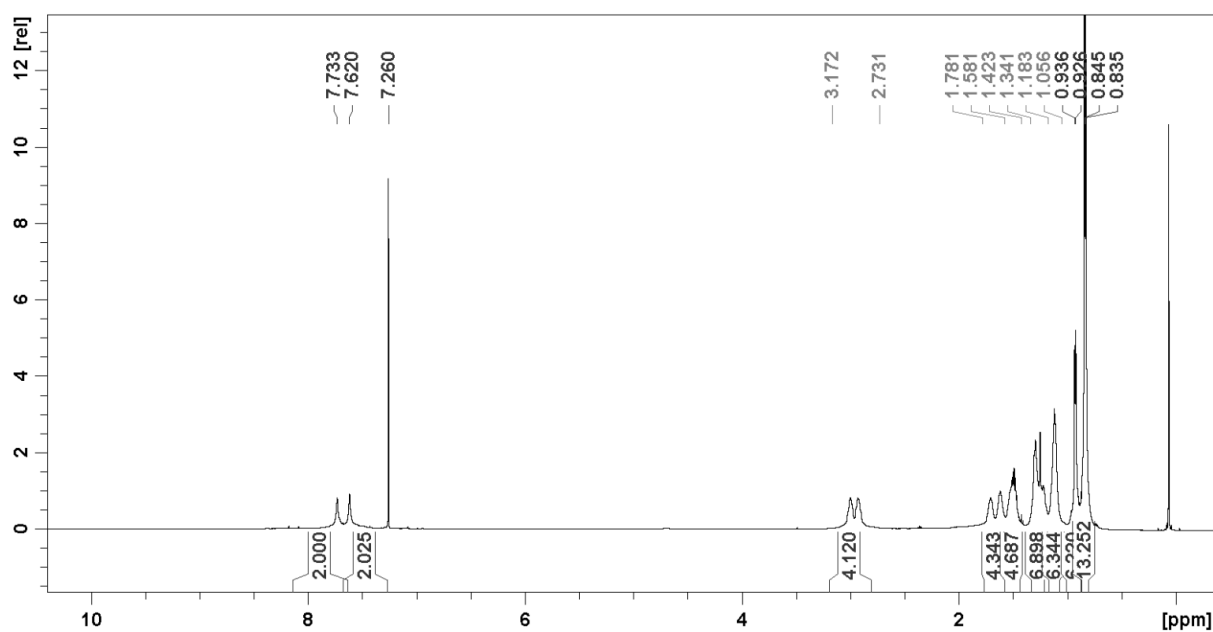


Figure S36: ^1H NMR spectrum (600 MHz, CDCl_3) of **4b**.

Polymers **5a** and **5b** did not dissolve sufficiently for NMR measurements in common solvents.

Significant broadening of the ^1H NMR signals of the aliphatic protons next to the sulfur atom was observed at higher concentrations for thioalkyl-substituted precursors, which may be attributed to strong intermolecular S \cdots S interactions.

3. Gel permeation chromatography (GPC)

An Agilent Technologies 1260 Infinity GPC System with 1260 RID and DAD VL was used for GPC measurements. Measurements were carried out at 80°C using analytical grade chlorobenzene as eluent with two PLgel 10 µm MIXED B columns in series. The molar mass as a function of elution time through the columns was calibrated using Agilent EasiVial narrow dispersity polystyrene standards. Samples were prepared by stirring the polymers in analytical grade chlorobenzene (~1-2 mg mL⁻¹) at 80°C overnight and filtering through VWR PES membrane 0.45 µm syringe filters before submission. Injection volume: 50 µL, flow rate: 1.00 mL min⁻¹, detection: DAD detector (due to low solubility of the polymers).

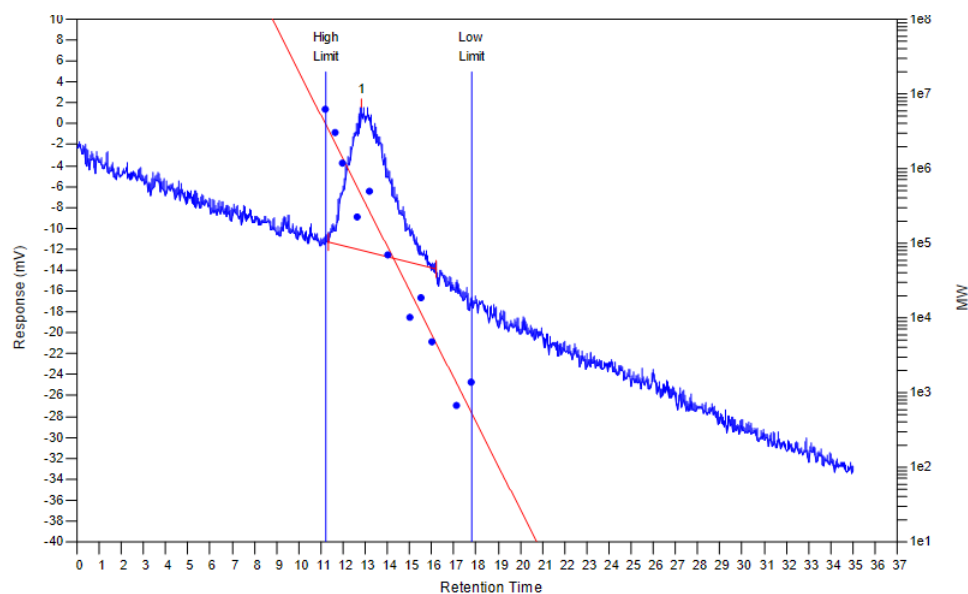


Figure S37: GPC measurement of polymer 4a.

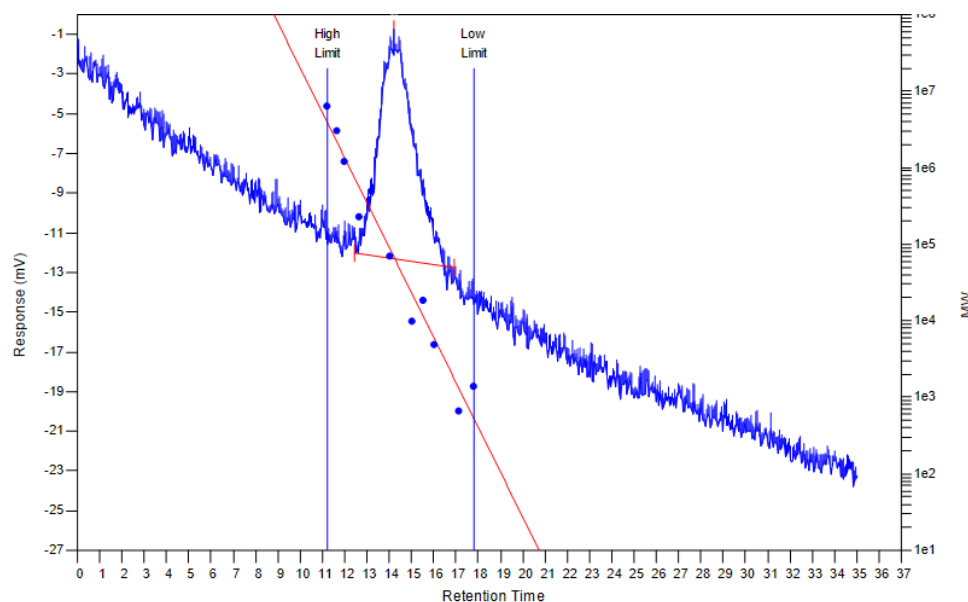


Figure S38: GPC measurement of polymer 4b.

4. Elemental analysis

Elemental analysis was carried out externally by Mag. Johannes Theiner at the University of Vienna. SO₂-PPVs **5a** and **5b** were heated to 200°C under N₂ flow for 2 min prior to elemental analysis to remove traces of entrapped solvent. ATR-FTIR spectra of the SO₂-PPVs did not change by the heat treatment. S-PPVs **4a** and **4b** were analysed without any pre-treatment.

5. Infrared (IR) spectra

Attenuated total reflection Fourier-transform infrared (ATR-FTIR) spectra were recorded on a Perkin Elmer Spectrum 2 working in ATR mode with a diamond crystal using Spectrum ST software for data collection and analysis. The resolution was set to 4 cm⁻¹ and spectra were recorded from 4000 to 600 cm⁻¹.

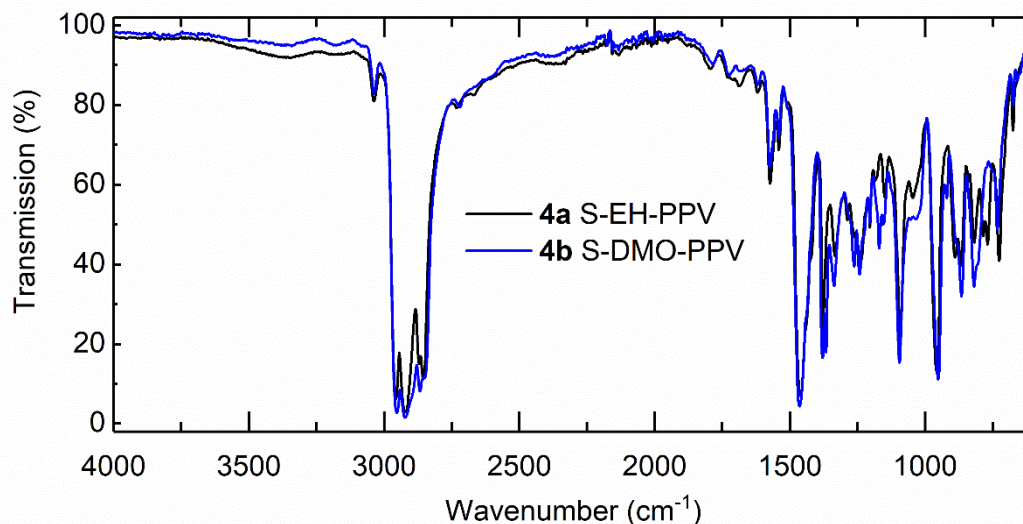


Figure S39: ATR-FTIR spectra of polymers **4a** and **4b**.

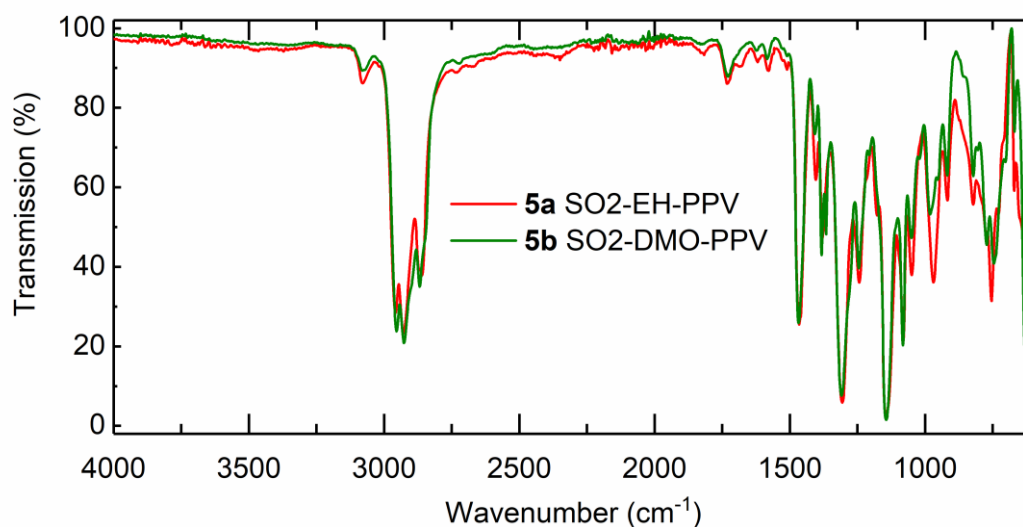


Figure S40: ATR-FTIR spectra of polymers **5a** and **5b**.

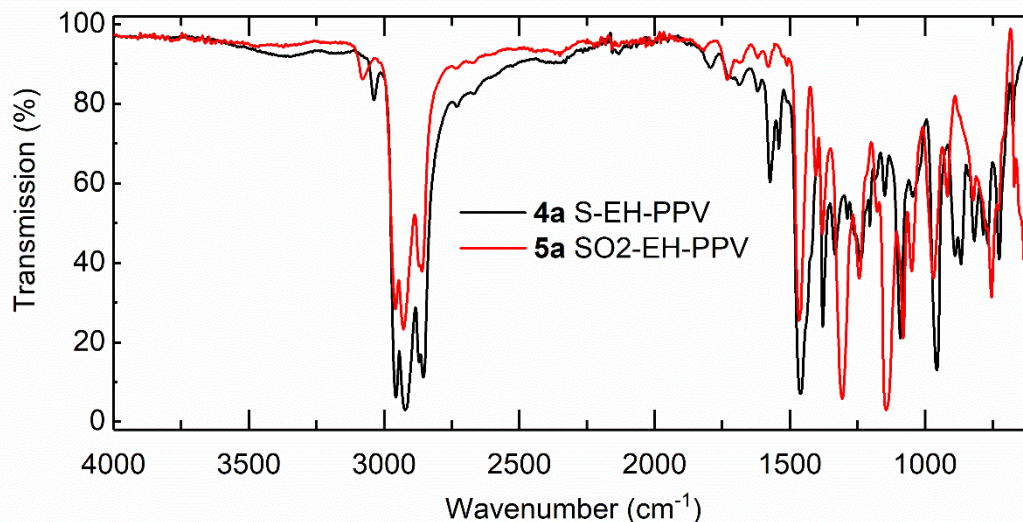


Figure S41: ATR-FTIR spectra of polymers **4a** and **5a**.

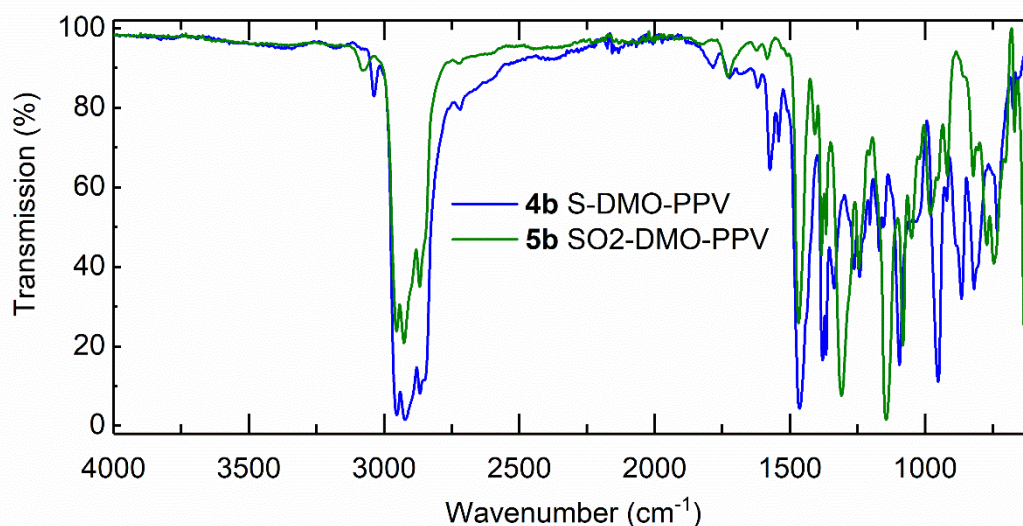


Figure S42: ATR-FTIR spectra of polymers **4b** and **5b**.

6. Thermogravimetric analysis (TGA) and differential scanning calorimetry (DSC)

TGA was carried out using a Perkin Elmer TGA 8000TM thermogravimetric analyzer. All measurements were performed under N₂ flow (10 mL/min) from 30°C to 900°C at a heating rate of 10°C/min. Pyris software was used for data collection and analysis. SO₂-PPVs **5a** and **5b** were heated to 200°C under N₂ flow for 2 min prior to the actual measurement to remove traces of entrapped solvent. ATR-FTIR spectra of the SO₂-PPVs did not change by the heat treatment. S-PPVs **4a** and **4b** were analysed without any pre-treatment.

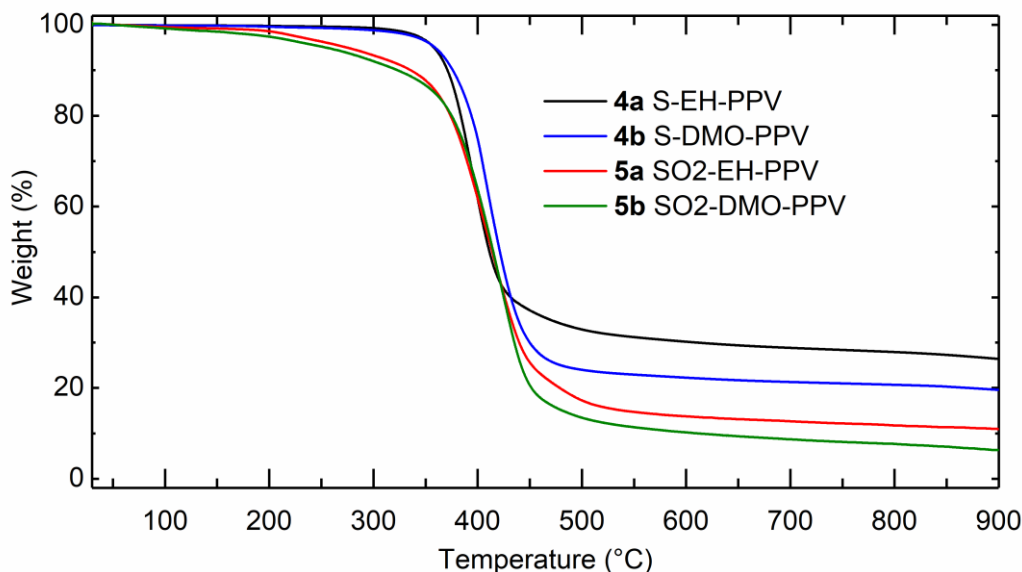


Figure S43: TGA curves of polymers **4a**, **4b**, **5a**, and **5b**.

DSC was performed on a Mettler Toledo DSC 823a at a heating rate of 10 °C/min, but the glass transition temperatures of the polymers could not be determined using this setup.

7. Cyclic voltammetry (CV)

Cyclic voltammetry (CV) measurements were carried out at room temperature using Metrohm Autolab B.V equipment (PGSTAT128N, differential electrometer amplifier). The measurements were performed at a scan rate of 0.02 Vs⁻¹. A three electrode configuration consisting of an indium tin oxide (ITO) working electrode, a platinum counter electrode, and a silver chloride coated silver reference electrode was used. The polymers were drop cast onto the ITO electrode from solutions in CHCl₃.

Ferrocene (Fc) in solution was measured as the reference compound. HOMO and LUMO levels of the polymers were deduced from the reduction and oxidation onset potentials on the premise that the Fc/Fc⁺ energy level is -4.80 eV. Tetrabutylammonium tetrafluoroborate (*n*-Bu₄NBF₄) in acetonitrile (0.1 M) was used as the supporting electrolyte. The supporting electrolyte solution was purged with nitrogen for 10 minutes prior to each measurement.

Polymer **5b** could not be measured due to insolubility in CHCl₃.

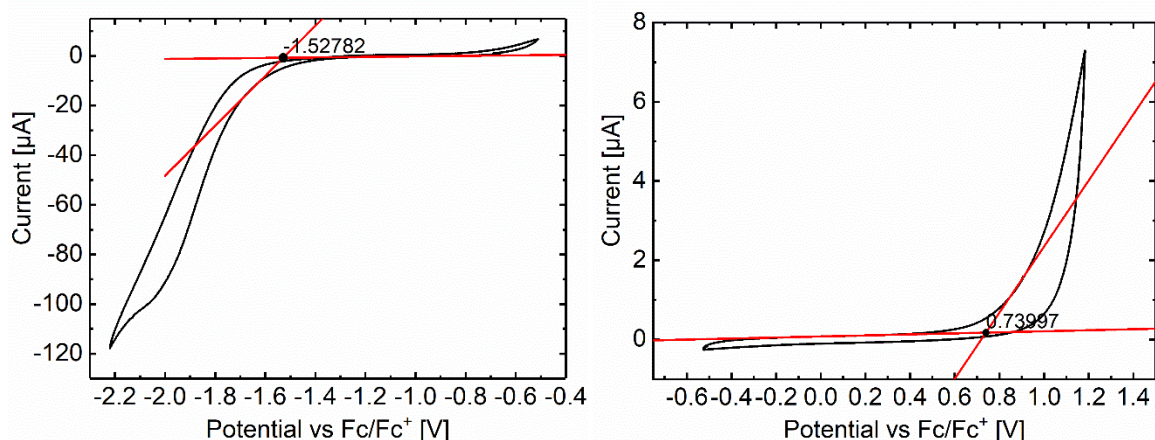


Figure S44: Cyclic voltammograms of drop-cast thin-films of polymer **4a**, reduction (left) and oxidation (right).

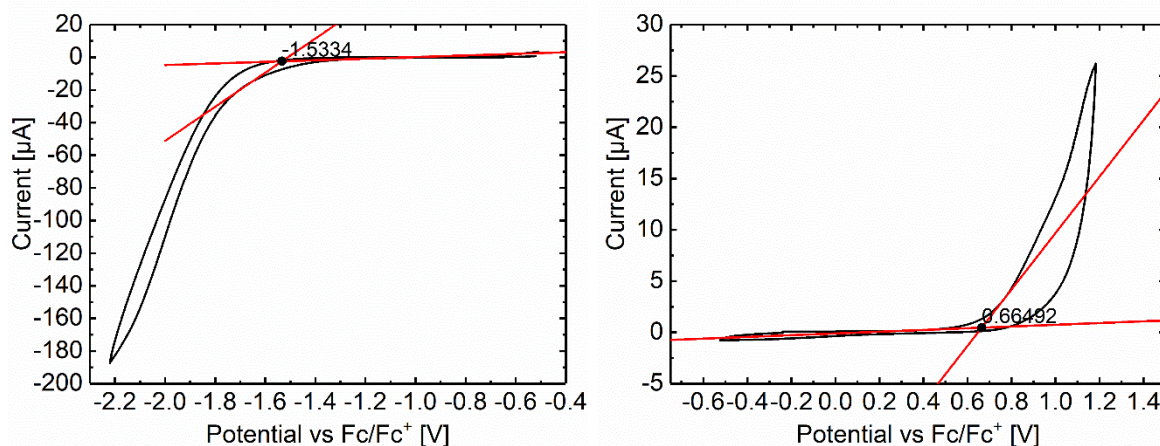


Figure S45: Cyclic voltammograms of drop-cast thin-films of polymer **4b**, reduction (left) and oxidation (right).

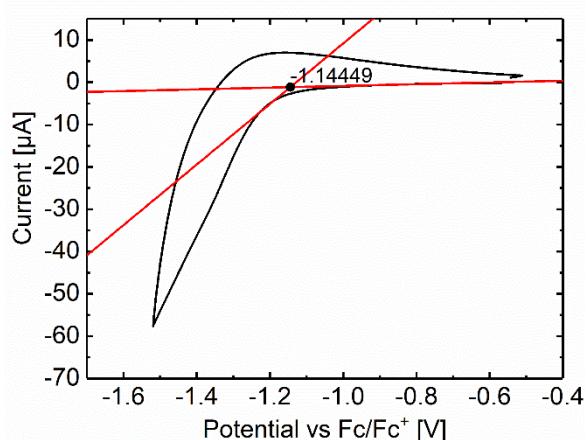


Figure S46: Cyclic voltammogram (reduction) of drop-cast thin-film of polymer **5a**.

8. Photophysical measurements

8.1. UV-vis absorption and photoluminescence (PL) in solution

Absorption spectra in solution were recorded at room temperature on a Perkin Elmer Lambda 750 spectrometer. The measurements were carried out in CHCl_3 at a repeat unit concentration of approx. $5 \mu\text{M}$. The measurements were repeated after storing the solutions under air and ambient light for 5 days to assess the photobleaching.

PL spectra in solution were recorded at room temperature on a PerkinElmer LS 55 spectrometer. The measurements were carried out in CHCl_3 at a repeat unit concentration of approx. $5 \mu\text{M}$, except for polymer **5a**, which had to be measured at a concentration of approx. $2.5 \mu\text{M}$ to avoid reaching the detector limit. Other measurement parameters: excitation wavelength: 450 nm; ExSlit: 2.5; EmSlit: 2.5; detector voltage: 650 (low gain).

Absorption and PL spectra of polymer **5b** in solution could not be measured, due to insolubility.

8.2. UV-vis absorption and photoluminescence (PL) spectra of thin-films

Thin-films were prepared by spin-coating dichlorobenzene solutions of the polymers on VWR Plain Micro Slides using a Laurell Model WS-650-23 spin coater under nitrogen atmosphere, with a 1000 rpm spin speed and 2 min spin time. The solutions were prepared by stirring the polymers in dichlorobenzene (5 mg mL⁻¹) at 120°C overnight. Small pieces that did not dissolve were avoided when pipetting the solutions.

Steady-state photoluminescence emission measurements were performed using a Horiba Scientific FluoroMax 4 spectrofluorometer.

8.3. Photoluminescence quantum efficiency (PLQE) in the solid state

Solid-state PLQE measurements were performed in the Horiba Quanta-Phi diffusely-reflecting integrating sphere attachment using the polymers as obtained after work-up. PLQE was calculated using the methodology detailed by Ahn et al.¹¹ The setup was calibrated by testing fluorescence standards Rhodamine 6G and Fluorescein to ensure the accuracy and reliability of calculated PLQE values.

Table 1: Overview of PLQE measurements of polymers **4a**, **4b**, **5a**, and **5b**.

	Excitation wavelength (nm)	Absorbance (%)	PLQE	Estimated error (±)
S-EH-PPV 4a	415	66	0.08	0.05
S-DMO-PPV 4b	480	45	0.05	0.05
SO ₂ -EH-PPV 5a (4.05 equiv DMDO)	415	69	0.36	0.05
SO ₂ -EH-PPV 5a (4.50 equiv DMDO)	415	48	0.19	0.05
SO ₂ -DMO-PPV 5b (4.05 equiv DMDO)	415	84	0.46	0.05
SO ₂ -DMO-PPV 5b (4.50 equiv DMDO)	415	55	0.23	0.05

9. Equation for DMDO concentration calculation

$$c_{DMDO} = \frac{n_t * (2 * \int_{2ox} + \int_{ox})}{(\int_{2ox} + \int_{ox} + \int_t) * v_{DMDO}}$$

c_{DMDO} ... concentration of DMDO in acetone (mol L⁻¹)

n_t ... amount of thioanisole (mmol) in used volume of thioanisole solution (1.00 mL)

\int_{2ox} ... ¹H NMR integral of sulfone CH₃ signal

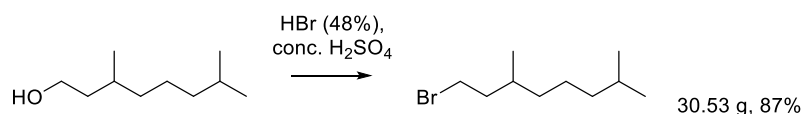
\int_{ox} ... ¹H NMR integral of sulfoxide CH₃ signal

\int_t ... ¹H NMR integral of thioanisole CH₃ signal

v_{DMDO} ... volume of used DMDO solution (0.25 mL)

10. Other syntheses

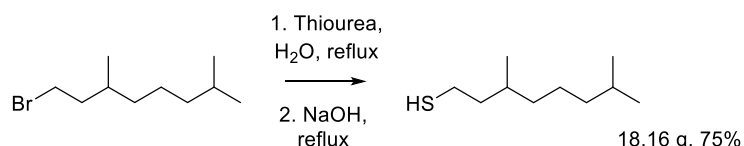
10.1. Synthesis of 1-bromo-3,7-dimethyloctane



Synthesis adapting a published protocol.¹²

48% HBr (25 mL) and conc. H₂SO₄ (14 mL) were heated to 120°C in a 100 mL flask. Starting at 60°C, 3,7-dimethyl-1-octanol (25.0 g, 157.9 mmol) was added slowly. The reaction was kept at 120°C overnight and was then allowed to cool to r.t. and extracted three times with petroleum ether (100 mL, 100 mL, 50 mL). The combined organic phases were washed with brine and dried over Na₂SO₄. The solvent was evaporated *in vacuo* and the crude product was purified by distillation under reduced pressure (6 mbar, boiling point approx. 87°C). 30.53 g (138.0 mmol, 87%) pure product were obtained.

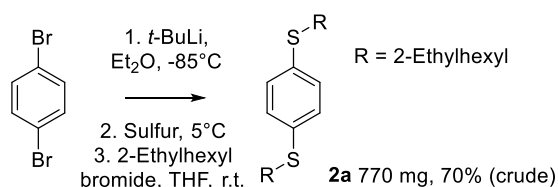
10.2. Synthesis of 3,7-dimethyl-1-octanethiol



Synthesis adapting a published protocol.¹³

A mixture of 1-bromo-3,7-dimethyloctane (30.53 g, 138.0 mmol, 1.0 equiv), thiourea (21.01 g, 276 mmol, 2.0 equiv), and water (8.6 mL) was heated to reflux overnight. NaOH (4.42 g) dissolved in 60 mL H₂O was then added and the reaction was kept at reflux for another 2 h. The reaction was then cooled to r.t. and extracted with petroleum ether three times (150 mL, 150 mL, 75 mL). The combined organic layers were dried over Na₂SO₄, the solvent was evaporated *in vacuo* and the crude product was purified by distillation under reduced pressure (7 mbar, boiling point approx. 85°C). 18.16 g (104.2 mmol, 75%) pure product were obtained.

10.3. Alternative synthesis of 1,4-dithioalkylbenzene 2a using *t*-BuLi and alkyl bromide



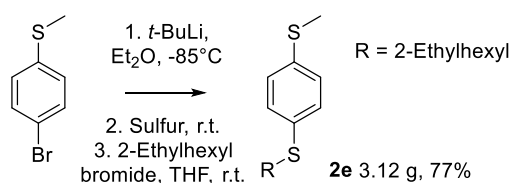
1,4-Dibromobenzene (708 mg, 3.0 mmol, 1.0 equiv) was dissolved in degassed dry Et₂O (15 mL, 0.2 M) under argon atmosphere in a 100 mL three-necked round bottom flask. The stirred solution was cooled to -85°C with a liquid N₂-acetone cooling bath and *t*-BuLi (7.1 mL, 1.7 M in pentane, 12.0 mmol, 4.0 equiv) was added slowly, so that the temperature did not rise above -65°C. The reaction was slowly warmed to 5°C within 3 h. Sulfur (212 mg, 6.6 mmol, 2.2 equiv) was then added and the resulting mixture was stirred for 40 min. 2-Ethylhexyl

bromide (1.74 g, 9.0 mmol, 3.0 equiv) and THF (15 mL) were then added and the reaction stirred at r.t. overnight.

For work-up, the reaction was extracted with water and the aqueous phase was extracted three times with Et₂O. The combined organic layers were dried over Na₂SO₄ and the solvent was removed *in vacuo* to yield 770 mg (2.1 mmol, 70%) crude product **2a** for further conversion.

The corresponding reactions using just either Et₂O or THF (instead of using Et₂O for the first step and then diluting with THF) failed.

10.4. Alternative synthesis of 1,4-dithioalkylbenzene **2e** using *t*-BuLi and alkyl bromide

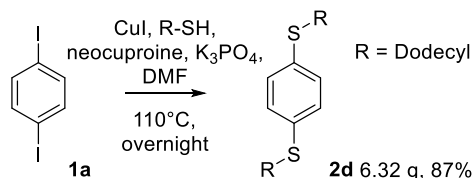


1-Bromo-4-(thiomethyl)benzene (3.05 g, 15.0 mmol, 1.0 equiv) was dissolved in degassed dry Et₂O (37.5 ml, 0.4 M) under argon atmosphere in a 250 mL three-necked round bottom flask. The stirred solution was cooled to -85°C with a liquid N₂-acetone cooling bath and *t*-BuLi (17.6 ml, 1.7 M in pentane, 30.0 mmol, 2.0 equiv) was added slowly, so that the temperature did not rise above -65°C. The resulting white slurry was slowly warmed to r.t. within 3 h. Sulfur (506 mg, 15.8 mmol, 1.05 equiv) was then added and the resulting suspension was stirred for 40 min. 2-Ethylhexyl bromide (3.77 g, 19.5 mmol, 1.3 equiv) and THF (37.5 mL) were then added and the reaction stirred at r.t. overnight.

For work-up, the reaction was extracted with water and the aqueous phase was extracted three times with Et₂O. The combined organic layers were dried over Na₂SO₄ and the solvent was removed *in vacuo*. The residue was purified by column chromatography (using petroleum ether as the eluent) and by subsequent evaporation of the solvent, yielding 3.12 g (11.6 mmol, 77%) slightly yellow product **2e**.

The corresponding reactions using just either Et₂O or THF (instead of using Et₂O for the first step and then diluting with THF) failed.

10.5. Alternative synthesis of 1,4-dithioalkylbenzene **2d** in DMF



1,4-Diiodobenzene **1a** (5.0 g, 15.2 mmol, 1.0 equiv), CuI (0.58 g, 3.04 mmol, 0.2 equiv), K₃PO₄ (13.2 g, 62.3 mmol, 4.1 equiv), and neocuproine (0.63 g, 3.04 mmol, 0.2 equiv) were dissolved/suspended in 100 mL dry DMF under argon atmosphere. 1-Dodecanethiol (6.77 g, 33.4 mmol, 2.2 equiv) was added and the stirred reaction was heated to 110°C overnight. The reaction was then cooled to r.t. and the resulting precipitate was filtered off and washed with water and ethanol. For purification, the solid was dissolved in CH₂Cl₂ and filtered over a

pad of silica using CH_2Cl_2 as eluent. The solvent was then evaporated *in vacuo* to yield 6.32 g (13.2 mmol, 87%) pure white powder **2d**.

10.6. Synthesis of S-PPV monomers **3e** and **3a** in sealed, pressure resistant vials

Dithioalkylbenzene **2e** (268 mg, 1.0 mmol, 1.0 equiv) and paraformaldehyde (PFA) (150 mg, 5.0 mmol, 5.0 equiv) were dissolved/suspended in 3 mL formic acid (0.33 M) in a pressure resistant vial. The reaction was heated to 70°C for 20 min, 2.3 mL HBr (30% in acetic acid) were then added and the reaction was kept at 70°C for 18 h. The reaction was allowed to cool to r.t. and poured into 20 mL water. The resulting precipitate was stirred for 10 min, filtered off, washed with methanol, and dried *in vacuo* to yield 288 mg (0.63 mmol, 63%) slightly yellow monomer **3e**.

The related synthesis of **3a** did not afford a precipitate when pouring into water and hence required extraction with CH_2Cl_2 . The crude product obtained by extraction required purification by column chromatography (using petroleum ether as eluent), affording monomer **3a** in yields of only 9%.

10.7. Synthesis of S-PPV monomer **3a** in acetic acid (instead of formic acid)

The synthesis was carried out following the general procedure for the synthesis of **3a-c** and **3e-h** but replacing formic acid by acetic acid. In contrast to the synthesis in formic acid, no precipitation was observed. Hence, the reaction was neutralized with aqueous NaHCO_3 solution and was then extracted with CH_2Cl_2 . The combined organic layers were dried over Na_2SO_4 and evaporated *in vacuo*. The yellow, highly viscous residue was analysed by ^1H NMR spectroscopy, which revealed that small amounts of starting material **2a** were still present, some **3a** was formed, but mainly single bromomethylated intermediate was obtained (Figure S47). Molar ratio (estimated from integrals): 1.00 (**3a**):2.34 (intermediate):0.14 (**2a**).

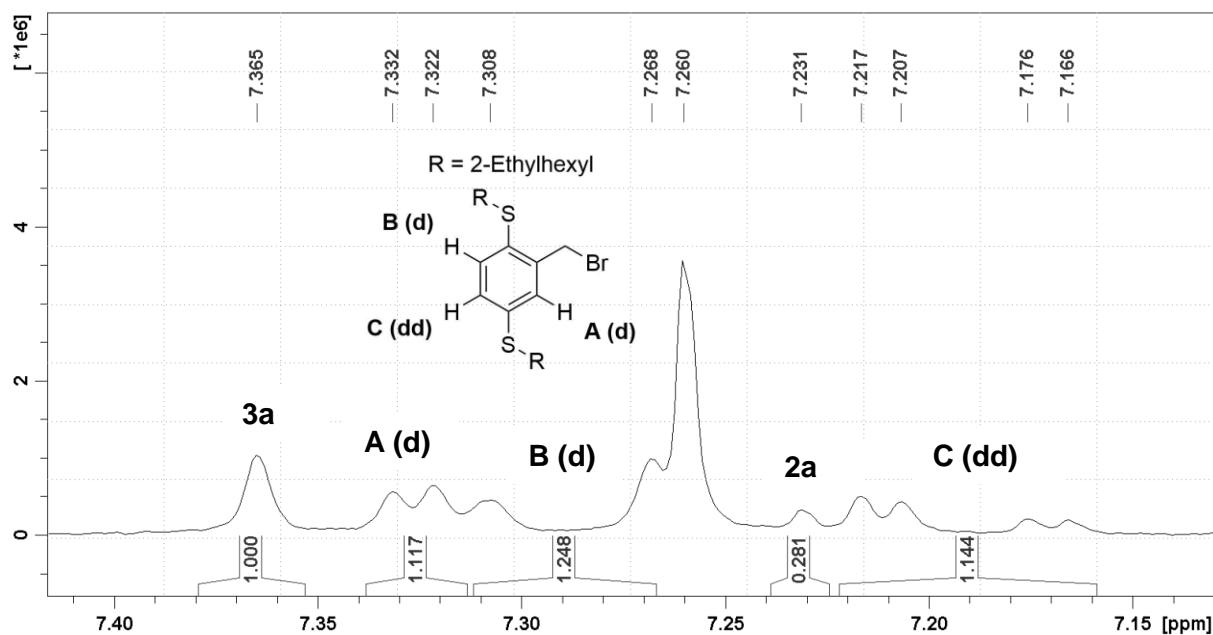
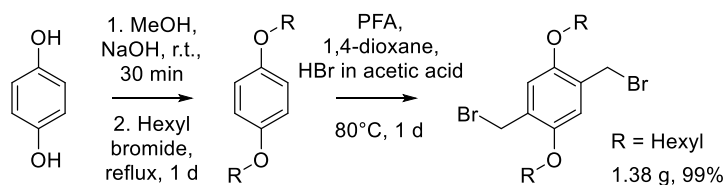


Figure S47: Aromatic region of the ^1H NMR spectrum of the product mixture obtained when testing the synthesis of monomer **3a** in acetic acid.

10.8. Synthesis of O-PPV monomers in 1,4-dioxane



In the first step, 1,4-dihexyloxybenzene was prepared from 1,4-dihydroxybenzene following a published procedure.¹⁴ For the second step, 1,4-dihexyloxybenzene (835 mg, 3.0 mmol, 1.0 equiv) and paraformaldehyde (PFA) (541 mg, 18.0 mmol, 6.0 equiv) were dissolved/suspended in 12 mL dry 1,4-dioxane (0.25 M) in a sealed vial with a septum. The mixture was purged with argon and 4.6 mL HBr (30% in acetic acid) were added dropwise. The resulting yellow solution was heated to 80°C for 1 d. The reaction was then cooled to r.t. for precipitation of the product, which was then filtered off and washed with water twice. After drying *in vacuo*, 1.38 g (3.0 mmol, 99%) pure double bromomethylated product was obtained. ¹H NMR (200 MHz, CDCl₃): 6.85 (s, 2H), 4.53 (s, 4H), 3.99 (t, *J* = 6.4 Hz, 4H), 1.91-1.70 (m, 4H), 1.61-1.22 (m, 12H), 1.00-0.81 (m, 6H) ppm. In accordance with the literature.¹⁵

11. Pictures of polymers 4a and 4b



Figure S48: Polymer 4a after precipitation from methanol and filtration.



Figure S49: Polymer **4a** after precipitation from methanol and filtration.

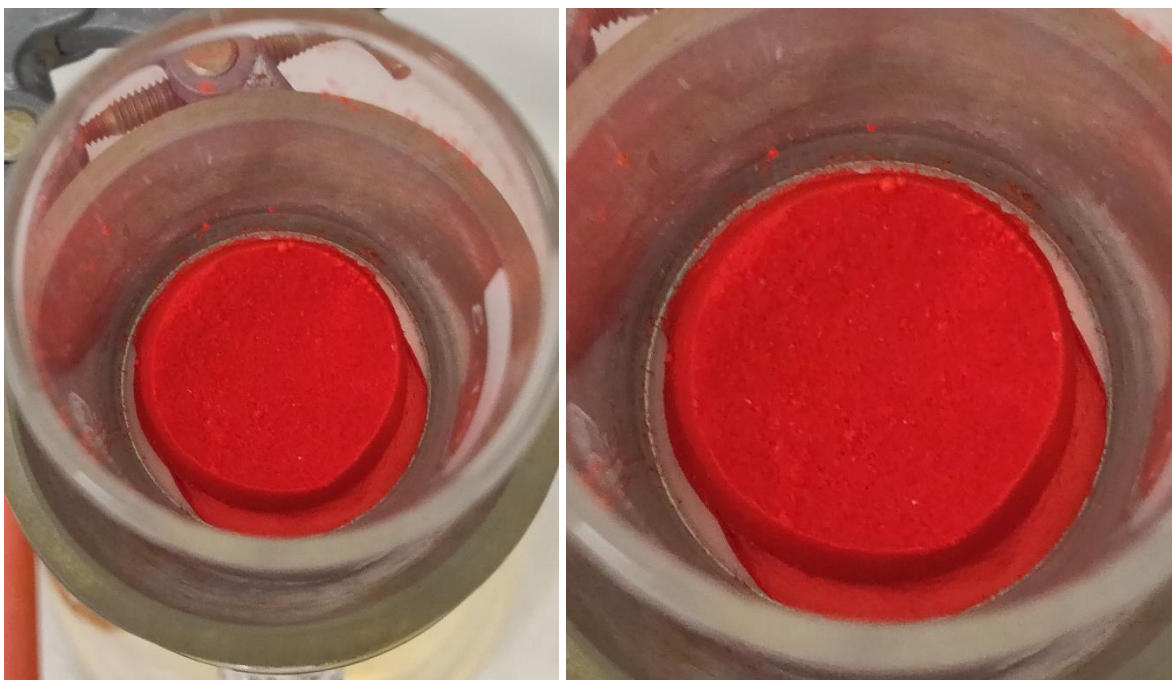


Figure S50: Polymer **4b** after precipitation from methanol and filtration.

12. Videos of post-polymerization modifications

Videos of the post-polymerization modifications of **4a** to **5a** and **4b** to **5b** are available on figshare: dx.doi.org/10.6084/m9.figshare.7277216. The videos show the addition of dimethyldioxirane (DMDO) in acetone to the polymers (dissolved in CHCl_3) as well as the rapid change of the photophysical properties within the first seconds of the reaction.

13. References

- 1 A. J. Blayney, I. F. Perepichka, F. Wudl and D. F. Perepichka, *Israel Journal of Chemistry*, 2014, **54**, 674-688.
- 2 O. Lhost and J. L. Brédas, *The Journal of Chemical Physics*, 1992, **96**, 5279-5288.
- 3 H. Kolshorn, H. Kretzschmann and H. Meier, *Journal für Praktische Chemie/Chemiker-Zeitung*, 1994, **336**, 292-296.
- 4 U. Stalmach, D. Schollmeyer and H. Meier, *Chemistry of Materials*, 1999, **11**, 2103-2106.
- 5 C.-B. Yoon, I.-N. Kang and H.-K. Shim, *Journal of Polymer Science Part A: Polymer Chemistry*, 1997, **35**, 2253-2258.
- 6 H. K. Shim, C. B. Yoon, T. Ahn, D. H. Hwang and T. Zyung, *Synthetic Metals*, 1999, **101**, 134-135.
- 7 J. Hou, B. Fan, L. Huo, C. He, C. Yang and Y. Li, *Journal of Polymer Science Part A: Polymer Chemistry*, 2006, **44**, 1279-1290.
- 8 F. H. Allen, C. M. Bird, R. S. Rowland and P. R. Raithby, *Acta Crystallographica Section B*, 1997, **53**, 696-701.
- 9 Q. J. Sun, J. H. Hou, C. H. Yang, Y. F. Li and Y. Yang, *Applied Physics Letters*, 2006, **89**, 153501.
- 10 C. Ton-That, G. Stockton, M. R. Phillips, T.-P. Nguyen, C. H. Huang and A. Cojocar, *Polymer International*, 2008, **57**, 496-501.
- 11 T.-S. Ahn, R. O. Al-Kaysi, A. M. Müller, K. M. Wentz and C. J. Bardeen, *Review of Scientific Instruments*, 2007, **78**, 086105.
- 12 C. Roche, H.-J. Sun, P. Leowanawat, F. Araoka, B. E. Partridge, M. Peterca, D. A. Wilson, M. E. Prendergast, P. A. Heiney, R. Graf, H. W. Spiess, X. Zeng, G. Ungar and V. Percec, *Nature Chemistry*, 2015, **8**, 80.
- 13 S. Vandeleene, K. Van den Bergh, T. Verbiest and G. Koeckelberghs, *Macromolecules*, 2008, **41**, 5123-5131.
- 14 J. P. Singh, U. Saha and T. H. Goswami, *Synthetic Metals*, 2012, **162**, 1240-1254.
- 15 J. M. Lucas, J. A. Labastide, L. Wei, J. S. Tinkham, M. D. Barnes and P. M. Lahti, *The Journal of Physical Chemistry A*, 2015, **119**, 8010-8020.